Neuropharmacology 233 (2023) 109548

Contents lists available at ScienceDirect

Neuropharmacology

journal homepage: www.elsevier.com/locate/neuropharm

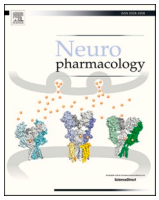

# Endocannabinoid-dependent decrease of GABAergic transmission on dopaminergic neurons is associated with susceptibility to cocaine stimulant effects in pre-adolescent male MAOA hypomorphic mice exposed to early life stress

Valeria Serra [a], Sonia Aroni [a], Marco Bortolato [b], Roberto Frau [a], Miriam Melis [a,*]

[a] Department of Biomedical Sciences, Division of Neuroscience and Clinical Pharmacology, University of Cagliari, 09042, Monserrato, Italy
[b] Department of Pharmacology and Toxicology, University of Utah, Salt Lake City, 84112, USA

ARTICLE INFO

Handling Editor: Dr M. Roberto

*Keywords:*
Cocaine
Dopamine
Early life stress
Endocannabinoid
MAOA
Ventral tegmental area

ABSTRACT

Vulnerability to cocaine use disorder depends upon a combination of genetic and environmental risk factors. While early life adversity is a critical environmental vulnerability factor for drug misuse, allelic variants of the monoamine oxidase A (MAOA) gene have been shown to moderate its influence on the risk of drug-related problems. However, data on the interactions between MAOA variants and early life stress (ES) with respect to predisposition to cocaine abuse are limited. Here, we show that a mouse model capturing the interaction of genetic (low-activity alleles of the *Maoa* gene; $MAOA^{Neo}$) and environmental (i.e., ES) vulnerability factors displays an increased sensitivity to repeated *in vivo* cocaine psychomotor stimulant actions associated with a reduction of GABAA receptor-mediated inhibition of dopamine neurons of the ventral tegmental area (VTA). Depolarization-induced suppression of inhibition (DSI), a 2-arachidonoylglycerol (2AG)-dependent form of short-term plasticity, also becomes readily expressed by dopamine neurons from male $MAOA^{Neo}$ ES mice repeatedly treated with cocaine. The activation of either dopamine D2 or CB1 receptors contributes to cocaine-induced DSI expression, decreased GABA synaptic efficacy, and hyperlocomotion. Next, *in vivo* pharmacological enhancement of 2AG signaling during repeated cocaine exposure occludes its actions both *in vivo* and *ex vivo*. This data extends our knowledge of the multifaceted sequelae imposed by this gene-environment interaction in VTA dopamine neurons of male pre-adolescent mice and contributes to our understanding of neural mechanisms of vulnerability for early onset cocaine use.

## 1. Introduction

Substance use disorders (SUD) are complex multifactorial conditions influenced by specific interactions among inheritable and environmental risk factors (Vink, 2016). Among the latter, exposure to early life stress (ES) represents an important environmental risk factor for the development of several neuropsychiatric disorders (e.g., depressive states, SUD) (Enoch, 2011; Hanson et al., 2021). ES increases the likelihood of developing SUD and lowers the age of initial drug use (Lo Iacono et al., 2018; Santo et al., 2021; Scheidell et al., 2018). Particularly, in the USA, most of SUD treatment admissions are aged 18 to 30, with ~10% initiated at 11 years or younger (Administration SAMHSA, 2014). In Europe, the average rate for students who begin using cocaine (or crack) at age 13 or younger is 0.4% (ESPAD, 2020). However, this developmental stage is an understudied subject, and sex/gender differences are often overlooked.

Individual genetic background also contributes to the onset and the progression of SUD (Fernàndez-Castillo et al., 2022; Kreek et al., 2005). Specific sets of genes involved in the mechanism of action of psychostimulants, particularly in the heavily-abused cocaine, are implicated in the development of this disorder, such as those related to monoamine neurotransmitters (Howell and Kimmel, 2008; Moeller et al., 2014). Among genetic factors, the monoamine oxidase A (MAOA) gene plays an important role (Stogner and Gibson, 2013; Vanyukov et al., 2007). MAOA is a key enzyme involved in monoamine degradation. Low-activity allelic variants of the *MAOA* gene (within a polymorphism with an upstream variable number of tandem repeat, uVNTR) are associated with an increased risk of drug abuse and dependence,

* Corresponding author.
*E-mail address:* myriam@unica.it (M. Melis).

https://doi.org/10.1016/j.neuropharm.2023.109548
Received 22 February 2023; Received in revised form 4 April 2023; Accepted 17 April 2023
Available online 18 April 2023

particularly when interacting with ES (Fite et al., 2018, 2020; Stogner and Gibson, 2013; Vanyukov et al., 2007). Cocaine users with low activity of MAOA show increased sensitivity to cocaine dependence across a lifetime, along with alterations in brain regions involved in reward processing, executive function and learning, key in SUD (Alia-Klein et al., 2011; Vanyukov et al., 2004, 2007; Verdejo-García et al., 2013). MAOA also plays an age-specific role in the etiopathogenesis of aggressive behavior (Yu et al., 2014), a trait increasing susceptibility to early-onset substance use (Brady et al., 1998; Miczek et al., 2004). Of note, a hypomorphic MAOA ($MAO^{Neo}$) mouse subjected to ES displays, at pre-adolescence, aggressive behavior associated with brain reward dopamine neurons exhibiting enhanced postsynaptic responsiveness to excitatory inputs (Frau et al., 2019a). Accordingly, an aberrant function of mesocorticolimbic dopamine pathway is associated with cross-sensitization between ES and cocaine exposure (Brake et al., 2004; Castro-Zavala et al., 2021; Enoch, 2011). The mesocorticolimbic dopamine system originates from cells within the ventral tegmental area (VTA) and mediates both natural rewards and the rewarding aspects of drugs of abuse (Morales and Margolis, 2017). Notably, the endocannabinoid system regulates dopamine neuronal activity, its influence on behavioral output (Melis and Pistis, 2012; Sagheddu et al., 2015) and individual susceptibility to SUD (Sagheddu and Melis, 2015). This latter includes, as an additional risk factor, a heightened motivational salience of reward cues displayed during adolescence (Luciana et al., 2012), which is associated with elevated dopamine signaling (Ernst and Luciana, 2015; Jordan and Andersen, 2016; McCutcheon et al., 2012; McCutcheon and Marinelli, 2009).

Despite this converging evidence, an unanswered question is whether individuals with a low *Maoa* gene activity who experienced ES display a vulnerability toward psychostimulant effects of cocaine. We, therefore, took advantage of a mouse model of this gene-environment (GxE) interaction, i.e. $MAO^{Neo}$ ES mouse (Godar et al., 2019), and subjected it to acute and repeated *in vivo* cocaine exposure. We used $MAO^{Neo}$ mice because they exhibit a low enzymatic brain MAOA activity (Bortolato et al., 2011), similar to humans with MAOA-uVNTR polymorphism(s) (Alia-Klein et al., 2008; Fowler et al., 1996, 2007; Shumay et al., 2012), whereas no functional VNTR *Maoa* polymorphisms have been documented in mice.

Here, we found that $MAO^{Neo}$ ES mice are hyper-responsive to psychostimulant effects of repeated *in vivo* cocaine exposure. This susceptibility is associated with synaptic changes at inhibitory afferents onto dopamine cells in the VTA. Such synaptic modifications involve the recruitment of a retrograde endocannabinoid signal and activation of dopamine D2 (DAD2) and type-1 cannabinoid (CB1) receptors, molecular targets exploited to prevent cocaine-induced increased hyperlocomotor effects.

## 2. Materials and methods

### 2.1. Animals

Male $MAOA^{Neo}$ mice were generated from 129S6 genetic background by mating primiparous $MAOA^{Neo}$ heterozygous females with wild-type (WT) sires, as previously described (Bortolato et al., 2011). Since *Maoa* is an X-linked gene, male offspring of $MAOA^{Neo}$ mice dams were either $MAOA^{Neo}$ or WT. Pregnant $MAOA^{Neo}$ mice were single-housed 3 days prior to parturition. Only litters with more than 4 pups (and at least 2 males) were used, and all litters with more than 8 pups were culled to 8 at postnatal day (PND) 1 to assure uniformity of litter size. Litter effects were minimized by using mice from at least six different litters for behavioral and electrophysiological experiments. Bedding was changed in all cages at PND 7 and PND 14, and mice were weaned at PND 21. Animals were grouped-housed in cages with food and water available *ad libitum*, except during the periods of social isolation, in which they were isolated in their home cage with *ad libitum* access to food (Teklad Global diets®) and water. The room was maintained at 22 °C, on a 12 h/12hr light/dark cycle from 7 a.m. to 7 p.m. Behavioral and electrophysiological experiments occurred between 10 a.m. and 6 p.m. during the light phase of the light/dark cycle. All procedures were performed in accordance with the European legislation (EU Directive, 2010/63) and were approved by the Animal Ethics Committees of the University of Cagliari and by Italian Ministry of Health (auth. n. 621/2016-PR). All efforts were made to minimize animal pain and discomfort and to reduce the number of animals used. Male $MAOA^{Neo}$ mice on 129S6 genetic background and their WT counterparts were used in this study. We limited the analyses to males for three main reasons: first, females do not display the hypomorphism, being the Maoa a X-linked gene. Second, it has been shown that the interaction between MAOA-L variants and early life stress in relation to externalizing behavior, including substance use and aggressive behavior, is mostly limited to males. Second, we found (Marco Bortolato unpublished data) that $MAOA^{Neo}$ homozygous females exposed to early-life stress exhibit a mild increase in aggression but only during the luteal phase of the estrous cycle. Conversely, no change was observed in estrous females.

### 2.2. Early stress procedures

To induce early life stress (ES), male pups were subjected to a daily regimen of maternal separation (MS) and saline injection, during the first postnatal week (from PND 1 to 7; Fig. 1A), as previously described (Frau et al., 2019a; Godar et al., 2019). Particularly, the timing of ES exposure was chosen based on the previously described behavioral outcome of this mouse model (Godar et al., 2019). At PND 22, mice were singly housed for 5 days before performing behavioral or electrophysiological experiments (Fig. 1A).

### 2.3. Assessment of locomotor activity

Locomotor activity was tested in motility chambers, consisting of a clear Plexiglas square arena (11 × 11 × 30 cm) covered by a clear Plexiglas plate, as previously described (Frau et al., 2019a). Basal locomotor activity was measured as total number of sequential infrared beam breaks in the horizontal sensor, recorded every 5 min. To evaluate the effect of cocaine on locomotor behavior, animals were first habituated to the apparatus for 15–30 min, then, after cocaine administration, locomotor activity was assessed for 120 min.

### 2.4. Ex vivo electrophysiology

The preparation of VTA slices was as described previously (Frau et al., 2019b). Briefly, horizontal midbrain slices (200 μm) were prepared 24 h after repeated cocaine *in vivo* exposure from $MAOA^{Neo}$ and WT mice (PND 28–30). VTA slice were prepared in ice-cold (4–6 °C) low-Ca2+ solution containing the following (in mM): 126 NaCl, 1.2 KCl, 1.2 NaH2PO4, 1.2 MgCl2, 0.625 CaCl2, 18 NaHCO3 and 11 glucose (304–306 mOsm). Immediately after cutting, slices were allowed to recover for at least 1 h at 36–37 °C until recording and superfused with artificial cerebrospinal fluid (aCSF) containing (in mM): 126 NaCl, 1.6 KCl, 1.2 NaH2PO4, 1.2 MgCl2, 2.4 CaCl2, 18 NaHCO3 and 11 glucose (304–306 mOsm). All solutions were saturated with 95% O2 and 5% CO2. Cells were visualized with an upright microscope with infrared illumination (Axioskop FS 2 plus; Zeiss), and whole-cell patch-clamp recordings were made by using an Axopatch 200B amplifier (Molecular Devices). Voltage-clamp recordings of evoked excitatory post-synaptic currents (EPSCs) were made with electrodes filled with a solution containing the following (in mM): 117 Cs methanesulfonic acid, 20 HEPES, 0.4 EGTA, 2.8 NaCl, 5 TEA-Cl, 2.5 Mg2ATP, and 0.25 Mg2GTP, pH 7.2–7.4, 275–285 mOsm. Picrotoxin (100 μm) was added to the aCSF to block GABAA receptor-mediated inhibitory post-synaptic currents (IPSCs). Voltage-clamp recordings of evoked IPSCs were made with electrodes filled with a solution containing the following (in mM): 144 KCl, 10 HEPES, 3.45 BAPTA, 1 CaCl2, 2.5 Mg2ATP and 0.25 Mg2GTP,

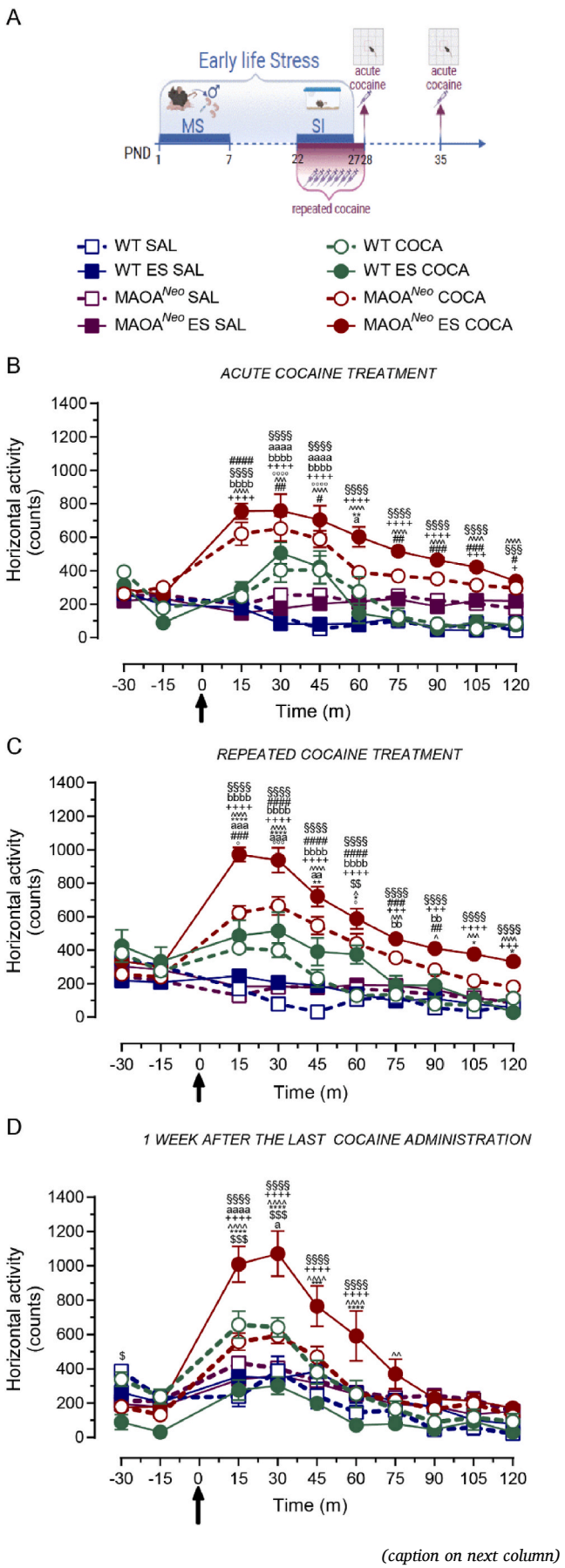


*(caption on next column)*

**Fig. 1.** Psychostimulant effects of cocaine in MAOA$^{Neo}$ mice subjected to early life stress. A Schematic experimental design to model early life stress (ES; see methods for maternal separation, MS, and social isolation, SI at different time windows; PND, post-natal day) and to evaluate the psychostimulant response to cocaine (COCA, 15 mg/kg, i.p.) or saline (10 ml/kg, i.p) after a single (PND28) and repeated exposure (PND 22–28), as well as after 1 week of withdrawal (PND 35). **B** Acute administration of cocaine increases the locomotor activity of MAOA$^{Neo}$ mice, in terms of horizontal activity and duration (Tukey's post hoc comparison: $^{\#\#\#\#}P < 0.0001$, $^{\#\#\#}P < 0.001$, $^{\#\#}P < 0.01$, $^{\#}P < 0.05$, $^{\S\S\S\S}P < 0.0001$, $^{\S\S\S}P < 0.001$, $^{aaaa}P < 0.0001$, $^{a}P < 0.05$, $^{bbbb}P < 0.0001$, $^{**}P < 0.01$, $^{\wedge\wedge\wedge\wedge}P < 0.0001$, $^{\wedge\wedge\wedge}P < 0.001$, $^{\circ\circ\circ\circ}P < 0.0001$, $^{++++}P < 0.0001$, $^{+}P < 0.05$. $n_{mice}$ = 14 WT SAL and WT ES SAL, 12 MAOA$^{Neo}$ SAL, 15 MAOA$^{Neo}$ ES SAL, 10 WT COCA and MAOA$^{Neo}$ COCA, 11 WT ES COCA, 13 MAOA$^{Neo}$ ES COCA). **C** Repeated exposure to cocaine for 1 week enhances the psychostimulant response to cocaine in MAOA$^{Neo}$ ES mice (Tukey's post hoc comparison: $^{\#\#\#\#}P < 0.0001$, $^{\#\#\#}P < 0.001$, $^{\#\#}P < 0.01$, $^{\S\S\S\S}P < 0.0001$, $^{aaa}P < 0.001$, $^{aa}P < 0.01$, $^{bbbb}P < 0.0001$, $^{bb}P < 0.01$, $^{****}P < 0.0001$, $^{**}P < 0.01$, $^{*}P < 0.05$, $^{\wedge\wedge\wedge\wedge}P < 0.0001$, $^{\wedge\wedge\wedge}P < 0.001$, $^{\wedge}P < 0.05$, $^{\circ\circ\circ}P < 0.001$, $^{\circ}P < 0.05$, $^{++++}P < 0.0001$, $^{+++}P < 0.001$, $^{\$\$}P < 0.01$. $n_{mice}$ = 11 WT SAL, 9 WT ES SAL, 12 MAOA$^{Neo}$ SAL and MAOA$^{Neo}$ ES SAL, 16 WT COCA and MAOA$^{Neo}$ COCA, 7 WT ES COCA, 19 MAOA$^{Neo}$ ES COCA). **D** The enhanced locomotor activity persists after 1 week from the last cocaine administration in MAOA$^{Neo}$ ES mice exposed to cocaine (Tukey's post hoc comparison: $^{\S\S\S\S}P < 0.0001$, $^{\$\$\$}P < 0.001$, $^{aaaa}P < 0.0001$, $^{a}P < 0.05$, $^{\wedge\wedge\wedge\wedge}P < 0.0001$, $^{\wedge\wedge}P < 0.01$, $^{****}P < 0.0001$, $^{***}P < 0.001$, $^{++++}P < 0.0001$. $n_{mice}$ = 9 WT SAL, 6 WT ES SAL, 12 MAOA$^{Neo}$ SAL, and MAOA$^{Neo}$ ES SAL, 6 WT ES COCA, 10 WT COCA and MAOA$^{Neo}$ COCA, 10 MAOA$^{Neo}$ ES COCA). Graphs show spontaneous locomotor (horizontal) activity measured as counts (bin = 15 min) in a motility chamber after saline or cocaine injection. The arrow indicates time of injection. Symbols on the graphs represent following comparisons: $^{\#}$WT COCA vs. MAOA$^{Neo}$ COCA, $^{\S}$WT COCA vs. MAOA$^{Neo}$ ES COCA, $^{\$}$WT COCA vs. WT ES COCA, $^{\wedge}$WT ES COCA vs. MAOA$^{Neo}$ ES COCA, $^{*}$MAOA$^{Neo}$ COCA vs. MAOA$^{Neo}$ ES COCA, $^{a}$WT COCA vs. WT SAL, $^{b}$MAOA$^{Neo}$ COCA vs. MAOA$^{Neo}$ SAL, $^{\circ}$WT ES COCA vs. WT ES SAL,$^{+}$MAOA$^{Neo}$ ES COCA vs. MAOA$^{Neo}$ ES SAL. Data are represented as mean ± SEM.

pH 7.2–7.4, 275–285 mOsm. All GABAA IPSCs were recorded in the presence of 6-cyano-2,3-dihydroxy-7- nitro-quinoxaline (10 μM) and 2-amino-5-phosphonopentanoic acid (AP5; 100 μM) to block AMPA and NMDA -receptors-mediated synaptic currents, respectively. Experiments were begun only after series resistance had stabilized (typically 15–40 MΩ). Series and input resistance were monitored continuously on-line with a 5 mV depolarizing step (25 ms). Data were filtered at 2 kHz, digitized at 10 kHz, and collected on-line with acquisition software (pClamp 10; Molecular Devices). Dopamine neurons from the lateral portion of the posterior VTA were identified by the following criteria (Frau et al., 2019b): cell morphology and anatomical location to the medial terminal nucleus of the accessory optic tract, the presence of a large hyperpolarization-activated current ($I_h$ size (pA): 208 ± 37 for WT; 186 ± 27 for MAOA$^{Neo}$; 201 ± 36 for WT ES; 185 ± 20 for MAOA$^{Neo}$ES) assayed immediately after break-in using 13 incremental 10 mV hyperpolarizing steps from a holding potential of −70 mV (Frau et al., 2019b). A bipolar, stainless steel stimulating electrode (FHC) was placed ~100–200 μm rostral to the recording electrode and was used to stimulate at a frequency of 0.1 Hz. Paired stimuli were given with an interstimulus interval of 50 ms, and the ratio between the second and the first post-synaptic currents (PSC2/PSC1) was calculated and averaged for a 5 min baseline (Melis et al., 2002). NMDA EPSCs were evoked while holding cells at +40 mV. The AMPA EPSC was isolated after bath application of the NMDA antagonist D-AP5 (100 μM). The NMDA EPSC was obtained by digital subtraction of the AMPA EPSCs from the dual (AMPA + NMDA-mediated) EPSC (Ungless et al., 2001). The values of the AMPA/NMDA ratio might be underestimated since the experiments were performed in the presence of spermine in the recording pipette. The depolarizing pulse used to evoke depolarization-induced suppression of inhibition (DSI) was a 3 s step to +40 mV from holding potential (Melis et al., 2009). This protocol was chosen on the evidence of a manifest endocannabinoid tone when VTA dopamine cells are held at + 40 mV for 3 s (Melis et al., 2004, 2009). The magnitude of DSI was

measured as a percentage of the mean amplitude of consecutive IPSCs after depolarization (acquired between 5 and 15 s after the end of the pulse) relative to that of baseline mean amplitude acquired before the depolarization (5 min). DSI peak magnitude was calculated as it follows: DSI (%) = 100 (1-$IPSC_{DSI}/IPSC_{baseline}$). It is thus possible to obtain negative values for DSI as a result, for example, of transient post-synaptic potentiation rather than DSI expression. Bath application of WIN55,212-2 (WIN) was performed as previously described (Frau et al., 2019b). The effect of JZL184 (100 nM) and AM281 (500 nM) on GABAA IPSCs was taken after 5 min bath application (Melis et al., 2013, 2014). Each hemi-slice received only a single drug exposure. All drugs were dissolved in dimethyl sulfoxide (DMSO) when it was needed. Particularly, AM281, JZL184, and WIN, 55,212-2 were dissolved in DMSO. The final concentration of DMSO was <0.001%, which was devoid of any effects.

### 2.5. Drugs and in vivo pharmacological treatment

Cocaine hydrochloride was purchased from Johnson Matthey; sulpiride was purchased from Teofarma; AM281 and JZL184 were purchased from Tocris Bioscience; WIN 55,212-2 was purchased from Sigma-Aldrich. Cocaine hydrochloride and sulpiride were dissolved in 0.9% saline solution, AM281 was dissolved in DMSO and saline solution (1:3 v/v). JZL184 was prepared as a saline:ethanol:cremophor (18:1:1 v/v/v) solution. All drugs were administered intraperitoneally (i.p.) in a volume of 10 ml/kg. Mice were given daily intraperitoneal injections of either saline (0.9% NaCl, 1 ml/kg) or cocaine (15 mg/kg) acutely or for 7 consecutive days (Fig. 1A). Pharmacological pretreatment with sulpiride, AM281 or JZL184 was carried out before cocaine administration and for 7 consecutive days. Doses were chosen based on previous studies (Aliczki et al., 2015; Cabib et al., 1991; Long et al., 2009; Pan et al., 2008; Vaseghi et al., 2012, 2013; Zhong et al., 2014) and by considering dose conversion between rat and mouse, and mouse and humans (Nair and Jacob, 2016). In order to minimize the number of animals used, *in vivo* pretreatment with one of these antagonists before saline injection was not carried out as it has been previously shown to not affect maximal IPSC amplitude, compared with that of saline injection alone (Pan et al., 2008).

### 2.6. Statistical analysis

All the numerical data are given as mean ± SEM. Statistical analysis was performed using GraphPad Prism (version 8). Statistical outliers were identified using Grubb's test ($\alpha = 0.05$) and excluded from analyses. Significance threshold was set at 95% confidence interval. With regard to behavioral experiments, data were compared and analyzed using mixed two-way ANOVA for repeated measures followed by Tukey's test for post hoc comparisons when the interaction between factors was revealed. Post hoc group differences within each time point are indicated by asterisks in the figures, but not described in the results. Electrophysiological data were compared and analyzed utilizing a two-way ANOVA, two-way ANOVA for repeated measures (treatment x time), or two-tailed Student's *t-test*, when appropriate, followed by Tukey's post hoc test comparisons when the interaction between factors was revealed. The significant threshold value was set at 0.05.

## 3. Results

### 3.1. Early life stress in hypomorphic MAOA mice increases cocaine-induced hyperlocomotion after repeated cocaine injections

Since aggressive behavior is a trait increasing susceptibility to early onset substance use (Brady et al., 1998; Miczek et al., 2004), we evaluated whether pre-adolescent (PND 28–30) $MAOA^{Neo}$ mice subjected to ES, which *per se* are aggressive (Frau et al., 2019a; Godar et al., 2019), could be hyper-responsive to psychomotor activating effects of cocaine (Fig. 1A). Only males underwent this investigation (see methods). Although $MAOA^{Neo}$ mouse background strain is not so responsive to cocaine as other mouse strains (Schlussman et al., 1998; Thomsen and Caine, 2011), $MAOA^{Neo}$ mice display an increased locomotor activity (Fig. 1B), after a single *in vivo* exposure to cocaine (15 mg/kg, i.p.), irrespective of ES (mixed two way RM ANOVA: time effect, $F(9,819) = 34.72$, $P < 0.0001$; group effect, $F(7,91) = 49.03$, $P < 0.0001$; interaction, $F(63,819) = 8.68$, $P < 0.0001$). However, repeated *in vivo* exposure to cocaine (7 days, once daily; Fig. 1C) unveils the GxE interaction (mixed two-way RM ANOVA: time effect $F(9,846) = 59.62$, $P < 0.0001$; group effect $F(7,94) = 45.84$, $P < 0.0001$; interaction $F(63,846) = 11.99$, $P < 0.0001$). Notably, this hyper-responsiveness to cocaine persisted after one week of withdrawal (Fig. 1D; mixed two-way RM ANOVA: time effect $F(9,603) = 83.51$, $P < 0.0001$; group effect $F(7,67) = 10.52$, $P < 0.0001$; interaction $F(63,603) = 6.63$, $P < 0.0001$).

### 3.2. Repeated in vivo cocaine exposure decreases GABAergic transmission onto dopamine cells

Repeated *in vivo* exposure to cocaine alters synaptic plasticity at excitatory synapses in the VTA, which plays an important role in behavioral consequences of cocaine use and abuse (Bellone et al., 2021; Borgland et al., 2004). To study the molecular mechanisms underlying the persistent hyper-responsiveness to *in vivo* cocaine effects (Fig. 1D), we measured the synaptic properties of VTA dopamine cells by performing whole-cell patch-clamp recordings in acute VTA slices in the absence of cocaine, i.e. 24 hr after the last cocaine administration (Fig. 2A,C) (Pan et al., 2008). We first recorded AMPA excitatory post-synaptic currents (EPSCs) from putative dopamine neurons and found no differences among groups in current-voltage relationships (Fig. 2B; two way ANOVA: group effect $F(3,63) = 0.42$, $P = 0.74$; mV effect $F(2,63) = 118.1$, $P < 0.0001$; interaction $F(6,63) = 0.17$, $P = 0.98$) and in the AMPA/NMDA ratio (Fig. 2C; two way ANOVA: gene effect $F(1,21) = 0.04$, $P = 0.85$; ES effect $F(1,21) = 2.86$, $P = 0.11$; interaction $F(1,21) = 0.11$, $P = 0.74$). Statistical analysis revealed a main effect of ES in NMDA EPSC decay time (Fig. 2D, two way ANOVA: gene effect $F(1,20) = 1.69$, $P = 0.21$; ES effect $F(1,20) = 10.39$, $P = 0.004$; interaction $F(1,20) = 0.13$, $P = 0.72$) and in the paired-pulse modulation (EPSC2/EPSC1) of AMPA EPSCs (Fig. 2E; two way ANOVA: gene effect $F(1,33) = 0.28$, $P = 0.6$; ES effect $F(1,33) = 5.66$, $P = 0.02$; interaction $F(1,33) = 0.02$, $P = 0.89$). Altogether, these data suggest that changes at excitatory inputs onto dopamine cells do not account for the enhanced responsiveness to cocaine exhibited exclusively by $MAOA^{Neo}$ ES mice upon repeated *in vivo* exposure to cocaine.

Since repeated *in vivo* cocaine exposure also diminishes GABA transmission in rat midbrain dopamine neurons (Bocklisch et al., 2013; Liu et al., 2005; Pan et al., 2008), we next examined the properties of GABA synaptic inputs on VTA dopamine neurons by recording GABAA IPSCs 24 h after the last cocaine administration (Fig. 3A).

$MAOA^{Neo}$ ES mouse dopamine cells exhibited a decreased maximal amplitude of GABAA IPSCs (Fig. 3B; mixed two-way RM ANOVA: stimulus intensity effect $F(3,90) = 43.91$, $P < 0.0001$; group effect $F(3,30) = 2.87$, $P = 0.048$; interaction $F(9,90) = 4.97$, $P = 0.008$), an effect accompanied by a paired-pulse facilitation of GABAA IPSCs (Fig. 3C; two way ANOVA: gene effect $F(1,47) = 7.53$, $P = 0.009$; ES effect $F(1,47) = 9.05$, $P = 0.004$; interaction $F(1,47) = 5.46$, $P = 0.024$). Both effects persisted after one week from the last cocaine administration (data not shown). Since basal inhibitory synaptic properties of VTA dopamine neurons of $MAOA^{Neo}$ mice are not affected by ES (Fig. 3D; stimulus intensity effect $F(3,48) = 40.39$, $P < 0.0001$; group effect $F(3,16) = 0.72$, $P = 0.55$; interaction $F(9,48) = 0.75$, $P = 0.659$; Fig. 3E; two way ANOVA: gene effect $F(1,17) = 2.21$, $P = 0.156$; ES effect $F(1,17) = 1.47$, $P = 0.241$; interaction $F(1,17) = 1.78$, $P = 0.199$), this reduced GABA efficacy on dopamine cells might be associated with the enhanced responsiveness to cocaine displayed by $MAOA^{Neo}$ ES mice. To test this possibility, we bath applied cocaine

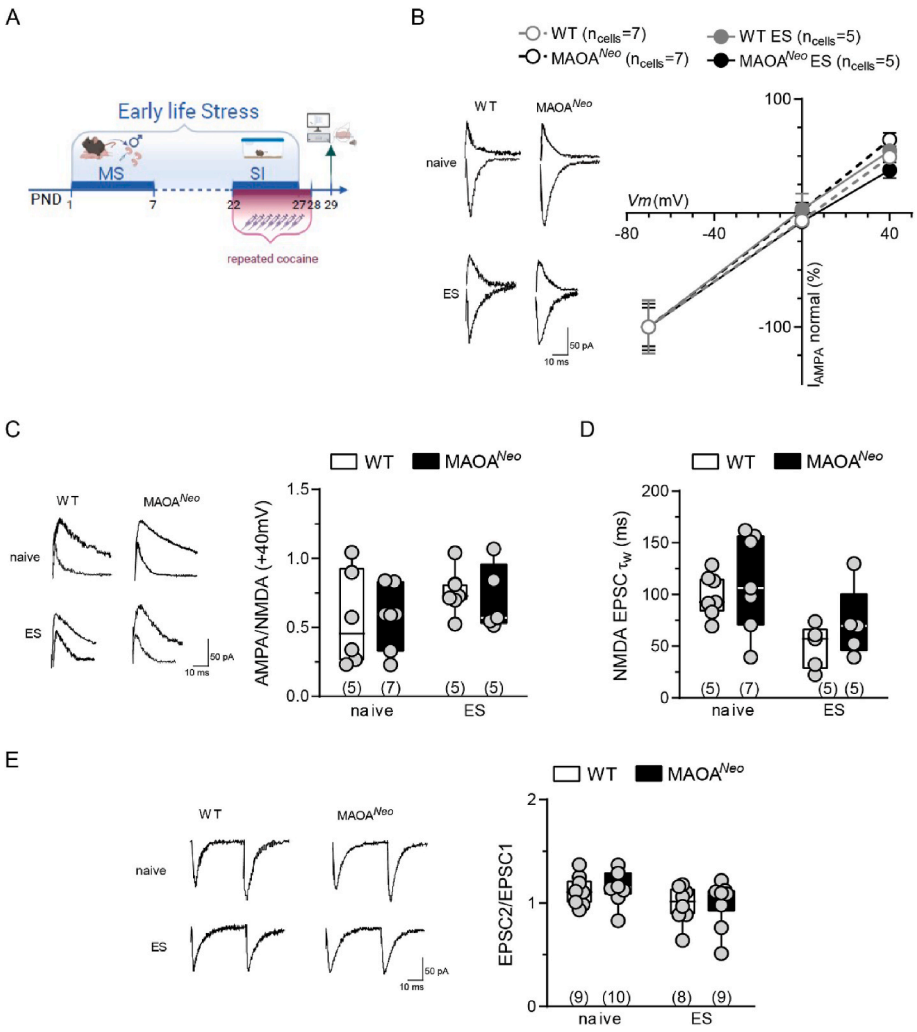


**Fig. 2.** Effect of repeated *in vivo* cocaine exposure on excitatory synaptic properties of VTA dopamine neurons in MAOA$^{Neo}$ ES mice. A Experimental design: WT and MAOA$^{Neo}$ mice were exposed to early life stress (ES; see methods for maternal separation, MS, and social isolation, SI at different time windows; PND, post-natal day). Mice were then administered cocaine (15 mg/kg i.p) for 1 week (PND 22–28) and subjected to whole cell patch clamp recordings 24 h after the last cocaine injection. **B** Current-voltage relationship (I–V) curves of AMPA EPSCs recorded from dopamine neurons in WT, WT ES and MAOA$^{Neo}$ ES ($n_{mice}$ = 5 per group), MAOA$^{Neo}$ ($n_{mice}$ = 7) mice. Insets show representative traces of AMPA EPSCs recorded at − 70 mV and +40 mV. Each symbol represents the averaged value (±SEM) obtained from different cells. **C** AMPA/NMDA ratio is not affected by repeated cocaine exposure in WT ($n_{cells}$ = 6), MAOA$^{Neo}$ and WT ES ($n_{cells}$ = 7 per group), MAOA$^{Neo}$ ES ($n_{cells}$ = 5) mice. Insets show representative traces of AMPA, and NMDA EPSCs recorded from dopamine neurons held at +40 mV in VTA slices. **D** Quantification of the data showing NMDAR EPSC decay time kinetics (weighted tau, τ) in WT and MAOA$^{Neo}$ ($n_{cells}$ = 7 per group), WT ES and MAOA$^{Neo}$ ES ($n_{cells}$ = 5 per group) slices. **E** Graph panel summarizing the effect of ES on paired-pulse ratio (EPSC2/EPSC1) of AMPA EPSCs recorded from WT ($n_{cells}$ = 9), MAOA$^{Neo}$ and MAOA$^{Neo}$ ES ($n_{cells}$ = 10 per group), WT ES ($n_{cells}$ = 8) slices. Insets show representative traces of paired AMPA EPSCs. Unless otherwise indicated, graphs show box-and-whisker plots (including minima, maxima and median values, and lower and upper quartiles) with each circle representing a single cell recorded (numbers in the brackets represent number of the mice).

(1–10 μM) to acute slices from animals repeatedly exposed to *in vivo* cocaine: in MAOA$^{Neo}$ ES mouse dopamine neurons, cocaine was almost twofold more potent and more effective in decreasing GABAA IPSC amplitude (Fig. 3F; mixed two way RM ANOVA: cocaine concentration effect F (2,40) = 71.07, P < 0.0001; group effect F (3,20) = 6.965, P = 0.002; interaction F (6,40) = 2.53, P = 0.0358).

In rats, cocaine-induced reduction of inhibitory strength on dopamine neurons depends on the recruitment of the endocannabinoid system (Pan et al., 2008). Of note, an endocannabinoid-dependent short-term form of synaptic plasticity, termed depolarization-induced suppression of inhibition (DSI), is associated with vulnerability to drugs of abuse (Melis et al., 2013, 2014; Tong et al., 2017). Therefore, we examined whether cocaine-exposed MAOA$^{Neo}$ ES mouse dopamine cells could express DSI at these synapses. We stimulated endocannabinoid synthesis and release by somatically injecting current into dopamine cells (Melis et al., 2004) and observed that MAOA$^{Neo}$ ES mouse dopamine neurons did not express DSI (Fig. 4A; mixed two-way RM ANOVA: time effect F (15,240) = 0.64, P = 0.83; group effect F (3,16) = 0.89, P = 0.46; interaction F (45,240) = 0.87, P = 0.69; Fig. 4B; two way ANOVA: gene effect F (1,16) = 1.63, P = 0.219; ES effect F (1,16) = 1.35, P = 0.26; interaction F (1,16) = 1.02, P = 0.327) unless subjected to repeated *in vivo* cocaine exposure (Fig. 5A–C; mixed two way RM ANOVA: time effect F (7.36,161.8) = 3.042, P = 0.0043; group effect F (3,22) = 5.683, P = 0.005; interaction F (45,340) = 1.37, P = 0.065; Fig. 5D; two way ANOVA: gene effect F (1,22) = 11.21, P = 0.003; ES effect F (1,22) = 7.4, P = 0.013; interaction F (1,22) = 10.25, P = 0.003). DSI was accompanied by an increased paired-pulse facilitation of these synapses after repeated *in vivo* cocaine exposure (Fig. 5E; Student's t-test: t (5) = 4.858, **P = 0.0046) and persisted after one week from the last cocaine administration (data not shown), suggestive of a decreased probability of GABA release (Melis et al., 2002).

Metaplastic changes in the molecular architecture of endocannabinoid system occurring in MAOA$^{Neo}$ ES mice repeatedly exposed *in vivo* to cocaine could explain DSI expression, particularly an enhanced endocannabinoid tone at these synapses. To assess this, we pharmacologically blocked CB1R in MAOA$^{Neo}$ ES mouse slices by bath applying the potent antagonist AM281 (500 nM, 5 min pre-incubation) (Fig. 6A), which *per se* did not alter GABAA IPSCs (two way ANOVA: F (1,18) = 1.91, P = 0.184) while prevented DSI (two way ANOVA: drug effect F (1,18) = 1.91, P = 0.184; depolarization effect F (1,18) = 10.81, P = 0.004; interaction F (1,18) = 9.31, P = 0.007). This suggests the absence of an endogenous cannabinoid tone in MAOA$^{Neo}$ ES mouse slices and confirms CBR1 role in DSI (Melis et al., 2014; Tong et al., 2017). Next, to test whether DSI could be ascribed to an increased CB1R function and/or number induced by repeated *in vivo* exposure to cocaine, we built a concentration-response relationship for the CB1R/CB2R agonist WIN55, 212-2 (WIN; 0.01–3 μM), but found no differences in the effect on evoked GABAA IPSCs amplitude recorded from VTA dopamine cells among groups (Fig. 6B; mixed two way ANOVA for repeated measures: group effect F (3,18) = 1.27, P = 0.364; concentration effect F (3.02, 52.6) = 34.58, P < 0.0001; interaction F (15,87) = 1.0, P = 0.459; Fig. 6C; mixed two way ANOVA for repeated measures: group effect F (3, 24) = 0.035, P = 0.99; time effect F (5.06,121.4) = 41.56, P < 0.0001; interaction F (102,816) = 0.67, P = 0.99). DSI in the VTA is mediated by

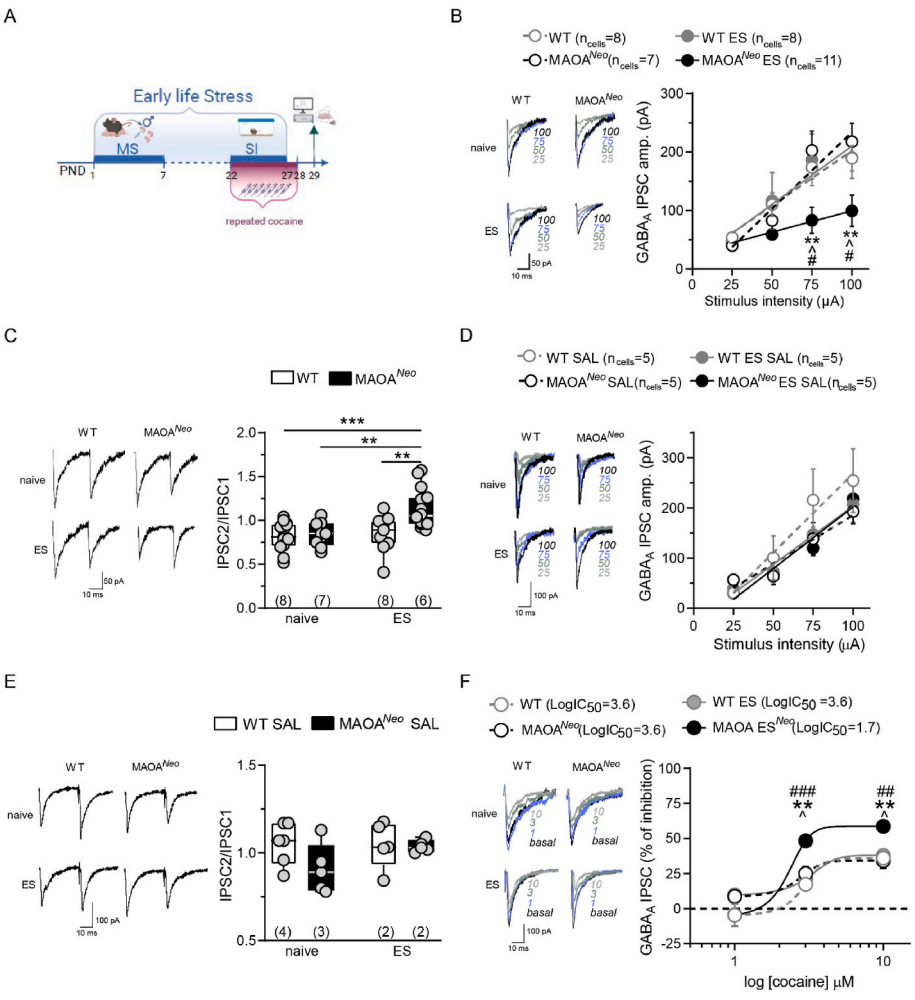


**Fig. 3.** Effect of repeated *in vivo* cocaine exposure on inhibitory transmission on VTA dopamine neurons in MAOA$^{Neo}$ ES mice. A Experimental design: WT and MAOA$^{Neo}$ mice were exposed to early life stress (ES; see methods for maternal separation, MS, and social isolation, SI at different time windows; PND, post-natal day). Mice were then administered cocaine (15 mg/kg i.p) for 1 week (PND 22–28) and subjected to whole cell patch clamp recordings 24 h after the last cocaine injection. **B** Input–output relationships of GABAA-mediated IPSCs from WT and WT ES ($n_{mice}$ = 8 per group), MAOA$^{Neo}$ ($n_{mice}$ = 7), and in MAOA$^{Neo}$ ES ($n_{mice}$ = 6) mouse dopamine neurons (Tukey's post hoc comparison: ** P < 0,01, MAOA$^{Neo}$ ES vs. MAOA$^{Neo}$; * P = 0,013, MAOA$^{Neo}$ ES vs. WT ES; * P = 0.014, MAOA$^{Neo}$ ES vs. WT). Each symbol represents the averaged value (±SEM) obtained from different cells. Insets shows representative traces of GABAA IPSCs recorded from dopamine neurons at each stimulus intensity. **C** Traces (*left*) and plots (*right*) of averaged paired-pulse ratio (IPSC2/IPSC1) of GABAA IPSCs of dopamine neurons recorded 24 h after the last treatment of repeated cocaine exposure in WT and WT ES ($n_{cells}$ = 13 per group), MAOA$^{Neo}$ ($n_{cells}$ = 9), and in MAOA$^{Neo}$ ES ($n_{cells}$ = 16) mice (Tukey's post hoc comparison: *** P = 0,0003, MAOA$^{Neo}$ ES vs. WT; ** P = 0,003, MAOA$^{Neo}$ ES vs. MAOA$^{Neo}$; ** P = 0.002, MAOA$^{Neo}$ ES vs. WT ES). Inset shows representative traces of paired GABAA IPSCs recorded from VTA putative dopamine neurons. **D** Input–output relationships of GABAA-mediated IPSCs from WT SAL ($n_{mice}$ = 4), MAOA$^{Neo}$ SAL ($n_{mice}$ = 3), WT ES SAL and MAOA$^{Neo}$ ES SAL ($n_{mice}$ = 2 per group) mouse dopamine cells. Each symbol represents the averaged value (±SEM) obtained from different cells. Insets show representative traces of GABAA IPSCs recorded at each stimulus intensity. **E** Graph panel summarizing the averaged paired-pulse ratio (IPSC2/IPSC1) of GABAA IPSCs for all cells recorded in WT SAL ($n_{cells}$ = 6), MAOA$^{Neo}$ SAL, WT ES SAL and MAOA$^{Neo}$ ES SAL ($n_{cells}$ = 5 per group) mice. Inset shows representative traces of paired GABAA IPSCs recorded from VTA putative dopamine neurons. **F** Dose–response curves for the inhibition of the GABAA IPSCs in cocaine-treated mouse slices by bath-application of cocaine (1, 3, 10 µM) displays a larger effect in MAOA$^{Neo}$ ES ($n_{cells,\ mice}$ = 5,5) than in WT ($n_{cells,\ mice}$ = 7,7), MAOA$^{Neo}$ ($n_{cells,\ mice}$ = 5,5) and WT ES ($n_{cells,\ mice}$ = 7,6) cells recorded 24 h after the last injection of repeated cocaine exposure (Tukey's post hoc comparison: 3 µM, ### P < 0.001, MAOA$^{Neo}$ ES vs. WT; ^ P < 0.05, MAOA$^{Neo}$ ES vs. MAOA$^{Neo}$; ** P < 0.01, MAOA$^{Neo}$ ES vs. WT ES; 10 µM, ## P < 0.01, MAOA$^{Neo}$ ES vs. WT; ^^ P < 0.01, MAOA$^{Neo}$ ES vs. MAOA$^{Neo}$; * P < 0.05, MAOA$^{Neo}$ ES vs. WT ES). Insets show IPSC traces recorded after 1 µM (blue), 3 µM (green), and 10 µM (grey) cocaine application. Each symbol represents the averaged value (±SEM) obtained from different cells. Unless otherwise indicated, graphs show box-and-whisker plots (including minima, maxima and median values, and lower and upper quartiles) with each circle representing a single cell recorded (numbers in the brackets represent number of the mice). (For interpretation of the references to colour in this figure legend, the reader is referred to the web version of this article.)

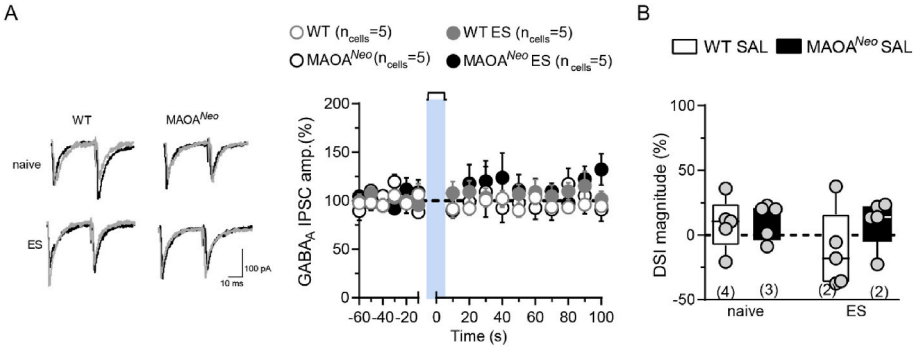


**Fig. 4.** MAOA$^{Neo}$ mouse dopamine neurons do not express depolarization-induced suppression of inhibition. A *Left panel* shows representative traces of IPSC recorded before (black) and after depolarization pulse (grey) recorded from VTA putative dopamine neurons. *Right panel* shows the time course of DSI in WT SAL ($n_{mice}$ = 4), MAOA$^{Neo}$ SAL ($n_{mice}$ = 3), WT ES SAL and MAOA$^{Neo}$ ES SAL ($n_{mice}$ = 2 per group) mouse dopamine neurons. GABAA IPSC amplitude was normalized to the averaged value (dotted line) before depolarization. Each symbol represents the averaged value (±SEM) obtained from different cells. **B** Graph shows box-and-whisker plots (including minima, maxima and median values, and lower and upper quartiles) with each circle representing a single cell recorded (numbers in the brackets represent number of the mice) of DSI peak magnitude expressed by VTA dopamine neurons in WT SAL, MAOA$^{Neo}$ SAL, WT ES SAL and MAOA$^{Neo}$ ES SAL ($n_{cells}$ = 5 per group) mice.

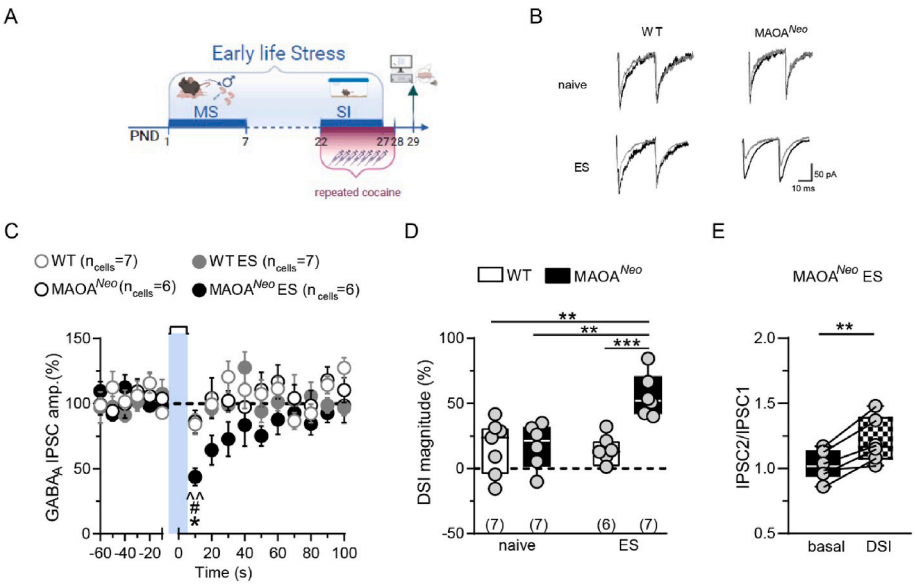


**Fig. 5.** Depolarization-induced suppression of inhibition is expressed in MAOA$^{Neo}$ ES mouse dopamine neurons after repeated *in vivo* cocaine exposure. A Experimental design: WT and MAOA$^{Neo}$ mice were exposed to early life stress (ES; see methods for maternal separation, MS, and social isolation, SI at different time windows; PND, post-natal day). Then mice were injected with cocaine (15 mg/kg i.p) for 1 week (PND 22–28) and subjected to whole cells patch clamp recordings 24 h after the last cocaine injection. **B** Representative traces of GABAA IPSCs recorded before (black) and after depolarization pulse (grey) recorded from VTA putative dopamine neurons after repeated *in vivo* cocaine exposure. **C** Graph panel showing the time course of DSI after repeated *in vivo* cocaine exposure. Application of a 3s depolarizing pulse on VTA dopamine neurons transiently reduces GABAA IPSC amplitude evoked by stimulating rostral afferents only in MAOA$^{Neo}$ ES mice (Tukey's post hoc comparison: 10 s, ^^P = 0.002, MAOA$^{Neo}$ ES vs. WT ES; #P = 0.011, MAOA$^{Neo}$ ES vs. WT; *P = 0.016, MAOA$^{Neo}$ ES vs. MAOA$^{Neo}$). GABAA IPSC amplitude was normalized to the averaged value (dotted line) before depolarization. Each symbol represents the averaged value (±SEM) obtained from different cells in WT ES ($n_{mice}$ = 6), WT, MAOA$^{Neo}$ and MAOA$^{Neo}$ ES ($n_{mice}$ = 7 per group). **D** Averaged data for DSI peak magnitude are plotted (Tukey's post hoc comparison: ***P < 0.001, MAOA$^{Neo}$ ES vs. WT ES; **P = 0.002, MAOA$^{Neo}$ ES vs. WT; **P = 0.003, MAOA$^{Neo}$ ES vs. ES). **E** Bar graph summarizing the averaged paired-pulse ratio (IPSC2/IPSC1) of rostral GABAA IPSCs for dopamine cells recorded before (basal) and after 3 s depolarization pulse (DSI) in MAOA$^{Neo}$ ES mice 24 h after the last day of repeated cocaine injection (Student's t-test: t (5) = 4.858, **P = 0.0046). Each symbol represents the averaged value (±SEM) obtained from different cells. Unless otherwise indicated, graphs show box-and-whisker plots (including minima, maxima and median values, and lower and upper quartiles) with each circle representing a single cell recorded (numbers in the brackets represent number of the mice).

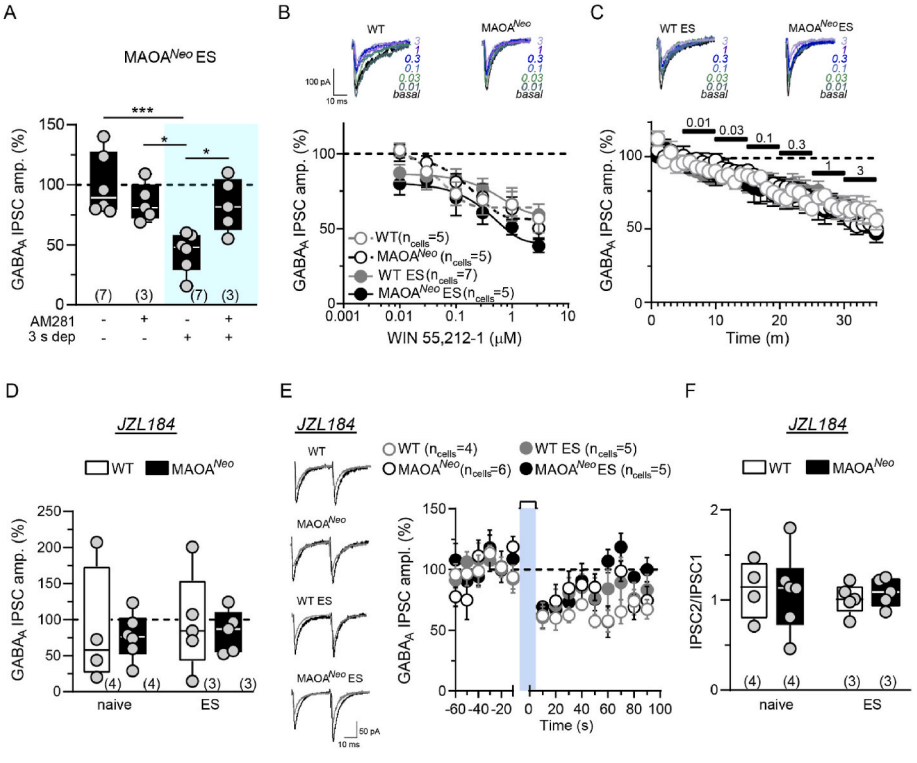


**Fig. 6.** DSI in MAOA$^{Neo}$ mouse VTA dopamine neurons after repeated cocaine exposure requires CB1R activation. A Bar graph summarizing the effect of CB1R antagonist AM281 (0.5 μM, 5 min) on GABAA IPSC amplitude in MAOA$^{Neo}$ ES mouse dopamine cells recorded 24 h after the end of repeated cocaine administration before and after the 3 s depolarizing pulse (Tukey's post hoc comparison: ***P < 0.001, *P < 0.05). **B** *Top*, Representative traces of GABAA IPSCs recorded from dopamine neurons in the absence (black) and the presence of WIN (0,01–3 μM). Dose–response curves for inhibition of GABAA IPSC amplitude by the CB1R agonist WIN55,212–2 as recorded from VTA dopamine cells in WT ($n_{mice}$ = 4), MAOA$^{Neo}$ ($n_{mice}$ = 2), WT ES ($n_{mice}$ = 6) and MAOA$^{Neo}$ ES ($n_{mice}$ = 5). **C** *Top,* Representative traces of GABAA IPSCs recorded from dopamine neurons in the absence (black) and the presence of WIN (0,01–3 μM). Time course of increasing concentrations of WIN on GABAA IPSC amplitude. Numbers on the chart above the bars indicate micromolar concentrations of WIN. Each symbol represents the averaged value (±SEM) obtained from different cells. **D** Bar graph displaying the effect of JZL184 (100 nM, MAGL inhibitor) on the amplitude of GABAA IPSCs recorded from WT ($n_{cells}$ = 4), MAOA$^{Neo}$ ($n_{cells}$ = 6), WT ES and MAOA$^{Neo}$ ES ($n_{cells}$ = 5 per group) mouse dopamine neurons. **E** Graph panel showing the time course of DSI in the presence of JZL184 in WT and MAOA$^{Neo}$ ($n_{mice}$ = 4 per group), WT ES and MAOA$^{Neo}$ ES ($n_{mice}$ = 3 per group) mouse dopamine neurons. GABAA IPSCs amplitude was normalized to the averaged value (dotted line) before depolarization. Each symbol represents the averaged value (±SEM) obtained from different cells. Insets show representative traces of IPSC recorded before (black) and after 3 s depolarization (grey). **F** MAGL inactivation abolishes differences in paired-pulse ratio (IPSC2/IPSC1) of rostral GABAA IPSCs for all dopamine cells recorded in WT ($n_{cells}$ = 4), MAOA$^{Neo}$ ($n_{cells}$ = 6), WT ES and MAOA$^{Neo}$ ES ($n_{cells}$ = 5 per group) mouse dopamine neurons. Unless otherwise indicated, graphs show box-and-whisker plots (including minima, maxima and median values, and lower and upper quartiles) with each circle representing a single cell recorded (numbers in the brackets represent number of the mice).

the endocannabinoid 2-arachidonoylglycerol (2AG) (Melis et al., 2013, 2014; Tong et al., 2017), whose half-life is often the rate-limiting step determining DSI magnitude and time course in the brain (Pan et al., 2009), including at inhibitory synapses in the VTA (Melis et al., 2013, 2014). Since 2AG half-life is tightly regulated by its main degrading enzyme monoacylglycerol lipase (MAGL) (Blankman et al., 2007), we next examined the effects of the MAGL inhibitor JZL184 on DSI. In the presence of JZL184 (100 nM, 5 min pre-incubation), which *per se* was ineffective (Fig. 6D; gene effect F (1,16) = 0.183, P = 0.674; ES effect F (1,16) = 0.109, P = 0.745; interaction F (1,16) = 0.003, P = 0.953), DSI was similarly expressed by all experimental groups (Fig. 6E; mixed two way ANOVA for repeated measures: group effect F (3,16) = 2.43, P = 0.102; time effect F (6.64,106.2) = 6.78, P < 0.0001; interaction F (42, 224) = 0.98, P = 0.496) along with their related paired-pulse facilitation (Fig. 6F; two way ANOVA: gene effect F (1,16) = 0.029, P = 0.865; ES effect F (1,16) = 0.158, P = 0.69; interaction F (1,16) = 0.13, P = 0.725). These results confirm the absence of a 2AG tone at these synapses in MAOA$^{Neo}$ ES mice repeatedly exposed *in vivo* to cocaine, and suggest a deficient clearance operated by MAGL, which could only be unveiled upon dopamine neuron depolarization. Our data also support that MAGL determines both the strength and the duration of retrograde synaptic signal (Melis et al., 2013, 2014; Pan et al., 2009; Santoni et al., 2023; Yoshida et al., 2011), being DSI expressed by dopamine cells in all experimental groups at a subthreshold duration of depolarization (3 s) in the presence of JZL184 (Fig. 5E), which abates endocannabinoid-dependent synaptic plasticity (Schlosburg et al., 2010), being DSI magnitude in MAOA$^{Neo}$ ES mice reduced in the presence of JZL184.

### 3.3. Dopamine and 2AG co-participate to depress GABAergic inputs on dopamine neurons

In the rat VTA, DAD2 receptor activation is implicated in 2AG synthesis and release from dopamine cells and in cocaine-induced decreased synaptic strength of GABA inputs (Pan et al., 2008b). We, therefore, investigated whether similar mechanisms were involved in

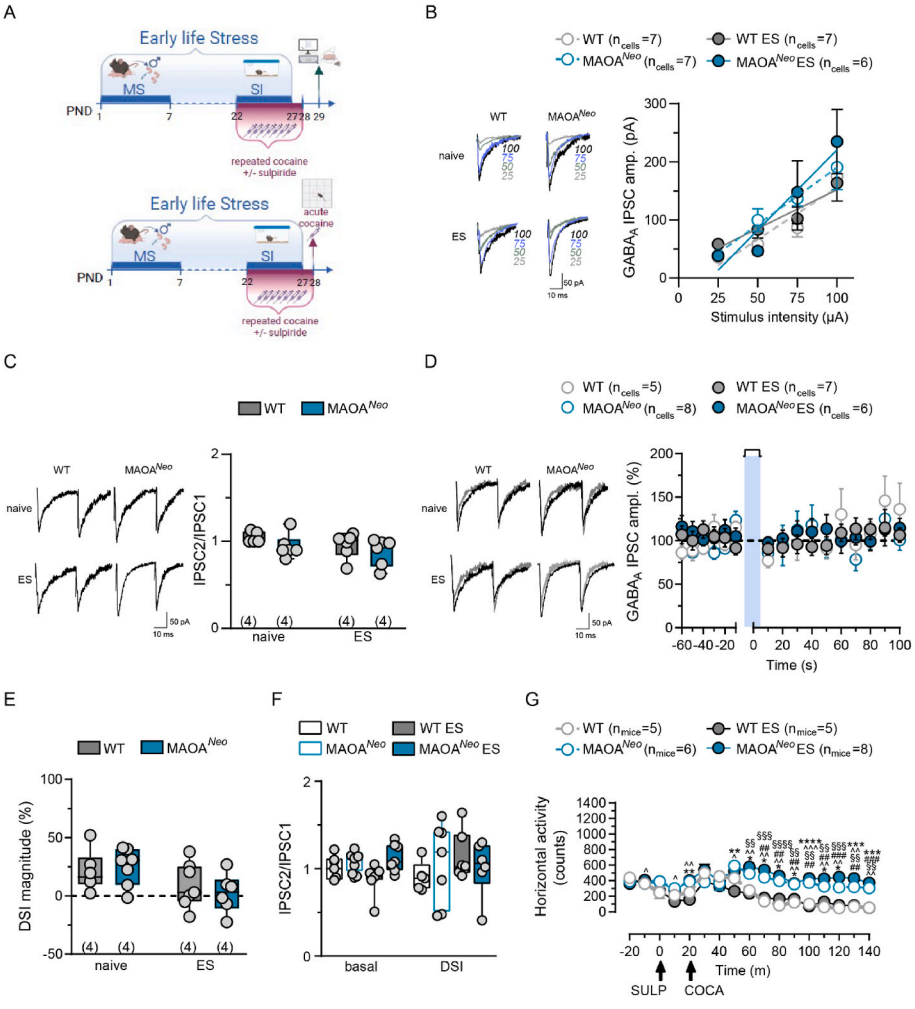


**Fig. 7.** *In vivo* pharmacological blockade of DA2D receptors restores synaptic properties and plasticity of inhibitory transmission on VTA dopamine neurons and prevents cocaine-induced hyperlocomotion in MAOA$^{Neo}$ ES mice. A *Top,* Experimental design: WT and MAOA$^{Neo}$ mice were exposed to early life stress (ES; see methods for maternal separation, MS, and social isolation, SI at different time windows; PND, post-natal day). The mice were injected with sulpiride (SULP, 10 mg/kg, i.p) 20 min before each cocaine injection (15 mg/kg i.p) for 1 week (PND 22–28) and subjected to whole cells patch clamp recordings 24 h after the last cocaine injection. *Bottom,* Experimental design: Same experimental timeline as above with the exception that on the last day of concomitant treatment mice were placed in the motility chamber to assess the locomotor activity. **B** SULP abolishes cocaine-induced reduction in the amplitude of GABAA IPSCs in MAOA$^{Neo}$ ES mouse dopamine neurons and differences among groups ($n_{mice}$ = 4 per group). Each symbol represents the averaged value (±SEM) obtained from different cells. Insets show representative traces of GABAA IPSCs recorded from dopamine neurons at each stimulus intensity. **C** Graph summarizing the effect of pretreatment with SULP on averaged paired-pulse ratio (IPSC2/IPSC1) for dopamine cells recorded in WT ($n_{cells}$ = 5), MAOA$^{Neo}$, WT ES and MAOA$^{Neo}$ ES ($n_{cells}$ = 6) mice. Inset shows representative traces of paired GABAA IPSCs recorded from VTA putative dopamine neurons. **D** *In vivo* pretreatment of SULP on time course of DSI in WT, MAOA$^{Neo}$, WT ES and MAOA$^{Neo}$ ES mouse dopamine neurons ($n_{mice}$ = 4 per group). *Left panel* shows representative traces of IPSCs recorded before (black) and after 3 s depolarization (grey). *Right panel* depicts time course of GABAA IPSC amplitude normalized to the averaged value (dotted line) before 3 s depolarization. Each symbol represents the averaged value (±SEM) obtained from different cells. **E** Averaged data for DSI peak magnitude are plotted. **F** Bar graph summarizing the averaged paired-pulse ratio (IPSC2/IPSC1) of GABAA IPSCs for all dopamine cells recorded after *in vivo* pretreatment with SULP, before (basal) and after 3 s depolarization (DSI). **G** SULP abolishes cocaine-induced hyperlocomotion in MAOA$^{Neo}$ ES mice (Tukey's post hoc comparison: $^{§§§§}$ P < 0.0001, **** P < 0.0001, $^{§§§}$ P < 0.001, $^{###}$ P < 0.001, $^{^^^}$ P < 0.001, *** P < 0.001, $^{§§}$ P < 0.01, $^{##}$ P < 0.01, $^{^^}$ P < 0.01, ** P < 0.01, $^{#}$ P < 0.05, $^{^}$ P < 0.05, * P < 0.05). Graph shows spontaneous locomotor (horizontal) activity measured as counts (bin = 10 min) before and after drug injection at the last day of repeated treatment in a motility chamber. Symbols on the graphs represent following comparisons: $^{§}$WT vs. MAOA$^{Neo}$ ES, $^{#}$WT vs. MAOA$^{Neo}$, $^{^}$WT ES vs. MAOA$^{Neo}$ ES, *WT ES vs. MAOA$^{Neo}$. Data are represented as mean ± SEM. Unless otherwise indicated, graphs show box-and-whisker plots (including minima, maxima and median values, and lower and upper quartiles) with each circle representing a single cell recorded (numbers in the brackets represent number of the mice).

cocaine-induced effects in MAOA$^{Neo}$ ES mice. Pharmacological *in vivo* pretreatment with the DAD2 receptor antagonist sulpiride (10 mg/kg, i.p., administered 20 min before cocaine administration for 7 consecutive days; Fig. 7A) resumed GABAergic transmission on VTA dopamine cells in terms of GABAA IPSC amplitude (Fig. 7B; mixed two way RM ANOVA: stimulus intensity effect F (3,69) = 38.61, P < 0.0001; group effect F (3, 23) = 0.64, P = 0.59; interaction F (9,69) = 1.30, P = 0.25) and paired-pulse ratio (Fig. 7C; two way ANOVA: gene effect F (1,19) = 2.47, P = 0.13; ES effect F (1,19) = 1.94, P = 0.17; interaction F (1,19) = 0.05, P = 0.82), abolished differences in the time course (Fig. 7D; mixed two way RM ANOVA: time effect F (6.53,143.7) = 2.16, P = 0.045; group effect F (3,22) = 0.18, P = 0.91; interaction F (45,330) = 1.01, P = 0.47) and magnitude of DSI (Fig. 7E; two way ANOVA: gene effect F (1,22) = 0.05, P = 0.82; ES effect F (1,22) = 6.26, P = 0.02; interaction F (1,22) = 0.611, P = 0.44) and its related paired-pulse facilitation (Fig. 7F; two way ANOVA: group effect F (3,42) = 0.53, P = 0.67; depolarization effect F (1,42) = 0.004, P = 0.95; interaction F (3,42) = 1.481, P = 0.23), as well as prevented cocaine-induced hyperlocomotion in MAOA$^{Neo}$ ES mice (Fig. 7G; mixed two way RM ANOVA: time effect F (6, 57, 144,6) = 15.03, P < 0.0001; group effect F (3,22) = 33.78, P < 0.0001; interaction F (48, 352) = 3.69, P < 0.0001).

Since DAD2 and CB1 receptors target the same downstream signaling pathway to reduce GABA release probability on dopamine neurons (Pan et al., 2008a,b), we next pharmacologically blocked *in vivo* CB1Rs by administering AM281 (2.5 mg/kg, i.p., administered 20 min before cocaine injection for 7 days; Fig. 8A). In MAOA$^{Neo}$ ES mice, this pre-treatment averted decreased GABA synaptic efficacy (Fig. 8B; mixed two way RM ANOVA: stimulus intensity effect F (3,66) = 27.81, P < 0.0001; group effect F (3,22) = 0.34, P = 0.79; interaction F (9,66) = 0.68, P = 0.71), differences in paired-pulse modulation (Fig. 8C; two way ANOVA: gene effect F (1,21) = 0.86, P = 0.36; ES effect F (1,21) = 0.37, P = 0.54; interaction F (1,21) = 1.43, P = 0.23), abolished differences in the time course (Fig. 8D; mixed two way RM ANOVA: time effect F (15,330) = 2.88, P = 0.0003; group effect F (3,22) = 1.26, P = 0.31; interaction F (45,330) = 0.624, P = 0.972) and magnitude of DSI (Fig. 8E; two way ANOVA: gene effect F (1,22) = 0.001, P = 0.96; ES effect F (1,22) = 0.05, P = 0.82; interaction F (1,22) = 0.04, P = 0.83) and its related paired-pulse facilitation (Fig. 8F; two way ANOVA: group

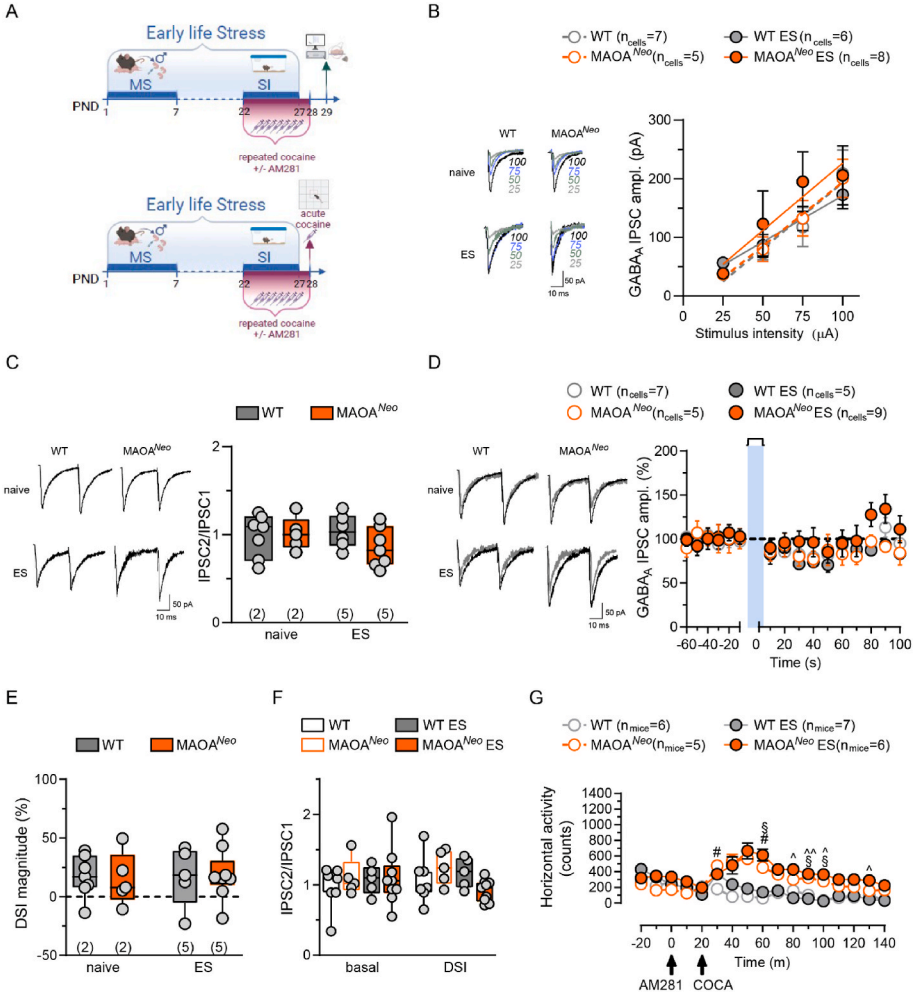


**Fig. 8.** *In vivo* pharmacological blockade of CB1R rescues synaptic properties and plasticity of inhibitory transmission on VTA dopamine neurons and normalizes cocaine-induced hyperlocomotion in MAOA$^{Neo}$ ES mice. A *Top,* Experimental design: WT and MAOA$^{Neo}$ mice were exposed to early life stress (ES; see methods for maternal separation, MS, and social isolation, SI at different time windows; PND, post-natal day). The mice were injected with AM281 (2.5 mg/kg, i.p) 20 min before each cocaine injection (15 mg/kg i.p) for 1 week (PND 22–28) and subjected to whole cell patch clamp recordings 24 h after the last cocaine injection. *Bottom,* Experimental design: Same experimental timeline as above with the exception that on the last day of concomitant treatment mice were placed in the motility chamber to assess the locomotor activity. **B** Input–output relationships of GABAA-mediated IPSCs recorded from VTA dopamine neurons. AM281 abolishes cocaine-induced differences among groups. ($n_{mice}$ = 2 for WT and MAOA$^{Neo}$; $n_{mice}$ = 5 for WT ES and MAOA$^{Neo}$ ES). Each symbol represents the averaged value (±SEM) obtained from different cells. Insets show representative traces of GABAA IPSC recorded at each stimulus intensity. **C** Graph summarizing the effect of *in vivo* pretreatment with AM281 on averaged paired-pulse ratio (IPSC2/IPSC1) for dopamine cells recorded from WT and MAOA$^{Neo}$ ES ($n_{cells}$ = 7 per group), WT ES ($n_{cells}$ = 6), MAOA$^{Neo}$ ($n_{cells}$ = 5) mice. Inset shows representative traces of paired GABAA IPSCs. **D** Graph panel showing the effect of *in vivo* pretreatment with AM281 on time course of DSI expressed by dopamine neurons in WT and MAOA$^{Neo}$ ($n_{mice}$ = 2 per group), WT ES and MAOA$^{Neo}$ ES ($n_{mice}$ = 5 per group) mice. GABAA IPSCs amplitude was normalized to the averaged value (dotted line) before depolarization. Each symbol represents the averaged value (±SEM) obtained from different cells. Insets show representative traces of IPSC recorded before (black) and after 3 s depolarization (grey). **E** Averaged data for DSI peak magnitude are plotted. **F** Bar graph summarizing the averaged paired-pulse ratio (IPSC2/IPSC1) of GABAA IPSCs for all dopamine cells recorded after *in vivo* pretreatment of AM281 before (basal) and after 3 s depolarization (DSI). **G** Cocaine-induced hyperlocomotion (Tukey's post hoc comparison: ^^ P < 0.01, $^{\S}$ P < 0.05, $^{\#}$ P < 0.05). Graph shows spontaneous locomotor (horizontal) activity measured as counts (bin = 10 min) before and after drugs injection at the last day of repeated treatment in a motility chamber. Symbols on the graphs represent following comparisons: ^WT ES vs. MAOA$^{Neo}$ ES, $^{\S}$WT vs. MAOA$^{Neo}$ ES, $^{\#}$WT vs. MAOA$^{Neo}$. Data are represented as mean ± SEM. Unless otherwise indicated, graphs show box-and-whisker plots (including minima, maxima and median values, and lower and upper quartiles) with each circle representing a single cell recorded (numbers in the brackets represent number of the mice).

effect F (3,44) = 1.015, P = 0.39; depolarization effect F (1,44) = 0.27, P = 0.60; interaction F (3,44) = 1.11, P = 0.38). AM281 also abolished cocaine-induced psychomotor effects in MAOA$^{Neo}$ ES mice (Fig. 8G; mixed two-way RM ANOVA: time effect F (7.15,143) = 13.77, P < 0.0001; group effect F (4,20) = 25.35, P < 0.0001; interaction F (48, 320) = 5.86, P < 0.0001). Finally, pharmacological *in vivo* MAGL inhibition (JZL 184: 8 mg/kg, i.p., administered 30 min before each cocaine injection for 7 consecutive days; Fig. 9A) restored GABA synaptic efficacy (Fig. 9B, mixed two way ANOVA for repeated measures: stimulus intensity effect F (3,96) = 49.95, P < 0.0001, group effect F (4,32) = 4.08, P = 0.008, interaction F (12,96) = 2.58, P = 0.005), differences in paired-pulse modulation (Fig. 9C; two way ANOVA: gene effect F (1,22) = 0.41, P = 0.53; ES effect F (1,22) = 5.48, P = 0.03; interaction F (1, 22) = 3.47, P = 0.08) and plasticity at inhibitory synapses on VTA dopamine cells MAOA$^{Neo}$ ES mice, including differences in the time course (Fig. 9D; mixed two way ANOVA for repeated measures: time effect F (15,405) = 6.75, P < 0.0001, group effect F (4,27) = 1.031, P = 0.409, interaction F (60,405) = 1.04, P = 0.396) and magnitude of DSI (Fig. 9E; two way ANOVA: gene effect F (1,22) = 0.011, P = 0.91; ES effect F (1,22) = 1.61, P = 0.22; interaction F (1,22) = 0.27, P = 0.61) and its related paired-pulse facilitation (Fig. 9F; two way ANOVA: group effect F (3,44) = 1.17, P = 0.33; depolarization effect F (1,44) = 6.85, P = 0.01; interaction F (3,44) = 1.011, P = 0.4), as well as their heightened locomotor responses to cocaine (Fig. 9G; mixed two way RM ANOVA: time effect F (4.525, 122.2) = 10.64, P < 0.0001; group effect F (3, 27) = 14.62, P < 0.0001; interaction F (51,459) = 4.93, P < 0.0001). Collectively, these results suggest that in MAOA$^{Neo}$ ES mice repeatedly treated with cocaine, DAD2 and CB1 receptors cooperate to diminish the strength of GABA transmission on VTA dopamine neurons and to enhance sensitivity to cocaine-induced hyperlocomotion.

## 4. Discussion

In the present study, we provide evidence that repeated *in vivo* exposure to cocaine produces an increase in its psychomotor stimulant effects especially in individuals whose susceptibility is driven by both genetic (MAOA$^{Neo}$) and environmental (ES) influences. The hyper-responsiveness to psychostimulant actions of cocaine exhibited by pre-

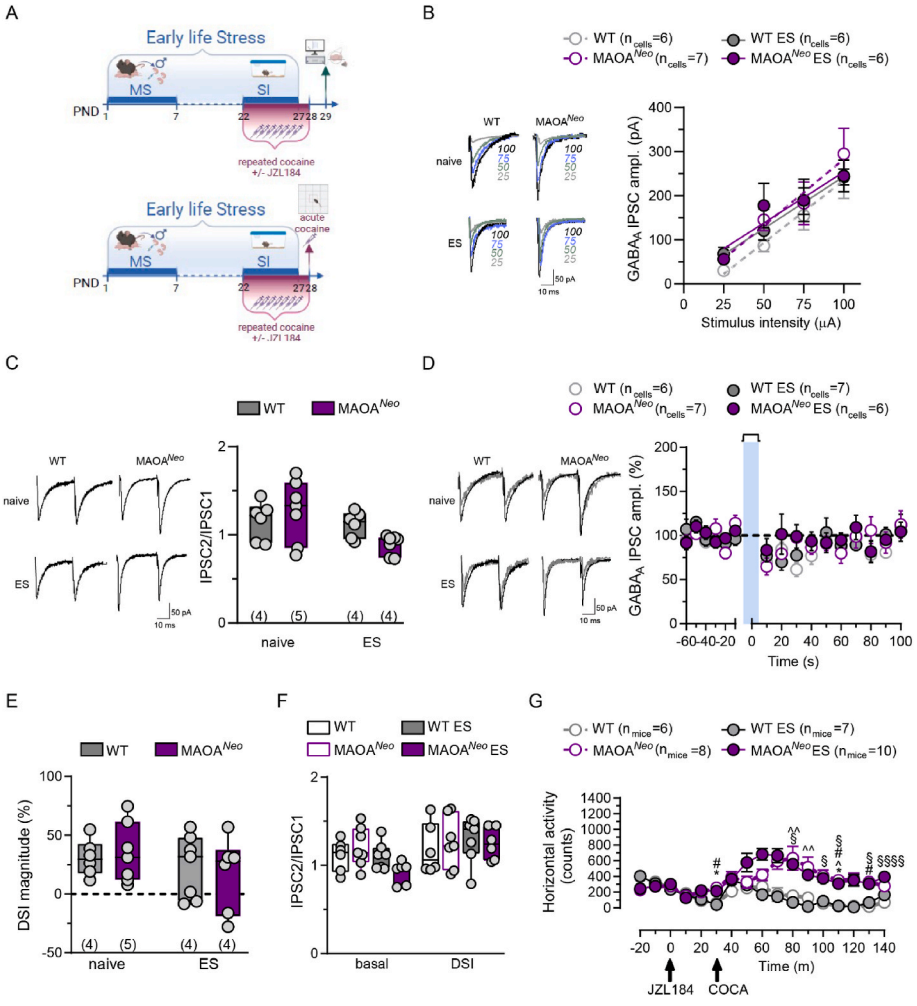


**Fig. 9.** *In vivo* pharmacological inhibition of MAGL restores synaptic properties and plasticity of inhibitory transmission on VTA dopamine neurons and reduces cocaine-induced hyperlocomotion in MAOA$^{Neo}$ ES mice. A *Top,* Experimental design: WT and MAOA$^{Neo}$ mice were exposed to early life stress (ES; see methods for maternal separation, MS, and social isolation, SI at different time windows; PND, postnatal day). The mice were injected with MAGL inhibitor, JZL184 (8 mg/kg, i.p) 30 min before each cocaine injection (15 mg/kg i.p) for 1 week (PND 22–28) and subjected to whole cell patch clamp recordings 24 h after the last cocaine injection. *Bottom,* Experimental design: Same experimental timeline as above with the exception that on the last day of concomitant treatment mice were placed in the motility chamber to assess the locomotor activity. **B** Input–output relationships of GABAA-mediated IPSCs recorded from dopamine neurons in MAOA$^{Neo}$ ($n_{mice}$ = 5), WT, WT ES and MAOA$^{Neo}$ES ($n_{mice}$ = 4 per group) mice. Each symbol represents the averaged value (±SEM) obtained from different cells. Insets show representative traces of GABAA IPSC recorded at each stimulus intensity. **C** Graph summarizing the effect of *in vivo* pretreatment with JZL184 on averaged paired-pulse ratio (IPSC2/IPSC1) for dopamine cells recorded from WT and WT ES ($n_{cells}$ = 6 per group), MAOA$^{Neo}$ and MAOA$^{Neo}$ES ($n_{cells}$ = 7 per group), mice. Inset shows representative traces of paired GABAA IPSCs recorded from VTA putative dopamine neurons. **D** Graph panel shows the effect of *in vivo* pretreatment with JZL184 on time course of DSI on VTA dopamine neurons from MAOA$^{Neo}$ ($n_{mice}$ = 5), WT, WT ES and MAOA$^{Neo}$ES ($n_{mice}$ = 4 per group) mice. GABAA IPSCs amplitude was normalized to the averaged value (dotted line) before depolarization. Each symbol represents the averaged value (±SEM) obtained from different cells. Insets show representative traces of IPSCs recorded before and after 3 s depolarization (grey). **E** Averaged data for DSI peak magnitude are plotted. **F** Bar graph summarizing the averaged paired-pulse ratio (IPSC2/IPSC1) of GABAA IPSCs recorded from all dopamine cells, before (basal) and after 3 s depolarization (DSI). **G** Cocaine-induced hyperlocomotion in MAOA$^{Neo}$ mice exposed to ES (Tukey's post hoc comparison: $^{§§§§}P < 0.0001$, ^^P < 0.01, $^{§}P < 0.05$, ^P < 0.05, *P < 0.05, $^{\#}P < 0.05$). Graph shows spontaneous locomotor (horizontal) activity measured as counts (bin = 10 min) before and after drugs injection at the last day of repeated treatment in a motility chamber arena. Symbols on the graphs represent following comparisons: $^{§}$WT vs. MAOA$^{Neo}$ ES, ^WT ES vs. MAOA$^{Neo}$ ES, $^{\#}$WT vs. MAOA$^{Neo}$, *WT ES vs. MAOA$^{Neo}$. Data are represented as mean ± SEM. Unless otherwise indicated, graphs show box-and-whisker plots (including minima, maxima and median values, and lower and upper quartiles) with each circle representing a single cell recorded (numbers in the brackets represent number of the mice).

adolescent male MAOA$^{Neo}$ ES mice is associated with adaptations specifically at inhibitory afferents on VTA dopamine neurons, an important locus of cocaine actions. These functional modifications relate to the interplay between dopamine and the endocannabinoid 2AG, key for the cross-sensitization of cocaine with environmental (ES) and genetic (MAOA$^{Neo}$) risk factors.

These findings support and extend previous studies showing that ES *per se* can enhance cocaine actions ((Vannan et al., 2018) and references therein), although this effect is often moderated by genetic factors (Fernàndez-Castillo et al., 2022). ES is a critical environmental risk factor for developing drug-related issues (Alves et al., 2020; Enoch, 2011; Fite et al., 2020; Vannan et al., 2018). In rodents, the use of maternal separation as a model of ES has provided important information about the mechanisms underlying susceptibility to drug misuse later in life (Castro-Zavala et al., 2020, 2021; Delavari et al., 2016; Ganguly et al., 2019; Vannan et al., 2018; Viola et al., 2016). Notably, dysregulated mesolimbic dopamine signaling has been associated with cross-sensitization between maternal separation and cocaine exposure (Brake et al., 2004; Castro-Zavala et al., 2021; Enoch, 2011). Accordingly, marked molecular alterations affect the responsiveness of dopamine neurons to subsequent exposure to stress and psychostimulants, and might predispose to the progression from cocaine use to abuse and dependence. This is particularly relevant when it occurs during vulnerable periods of life (Brake et al., 2004; Castro-Zavala et al., 2020, 2021; Delavari et al., 2016; Ganguly et al., 2019; Vannan et al., 2018; Viola et al., 2016). Our results support the evidence that predisposing risk factors, including pre-existing conditions (e.g., aggressive behavior), may lead to early onset drug use (Enoch, 2011; Jordan and Andersen, 2016; Mannuzza et al., 2008; Verdejo-García et al., 2013), associated with the highest risk of developing a SUD (Administration SAMHSA, 2018; Grant, 1998; Grant and Dawson, 1998). Our findings are consistent with the concept that sensitive developmental periods apply to SUD (Andersen, 2005) and that pinpointing neurobiological difference(s) between individuals biologically at risk, and those not at risk, for drug misuse, may provide molecular underpinnings that could be exploited as effective strategies to prevent the development of this brain disorder.

Our data substantiate the notion that not all individuals who experience ES will develop mental illness, particularly SUD, and highlight the role of other contributing factors in worsening one's lifetime trajectory, such as GxE interactions (Vink, 2016). Accordingly, among several genes implicated in susceptibility to SUD, those related to monoamines serve important roles (Howell and Kimmel, 2008; Volkow et al., 2007), particularly when associated with ES (Amsterdam et al., 2006; Lea and Chambers, 2007). Altogether, low-activity of *MAOA* genetic variants and lifetime stress enhance the risk for early experimentation with abused drugs (Fite et al., 2018, 2020; Stogner and Gibson, 2013; Vanyukov et al., 2004, 2007), besides the one for aggressive behavior (Caspi et al., 2002; Checknita et al., 2015; Guo et al., 2008; Viding and Frith, 2006; Weder et al., 2009). Here, we propose that the MAOA$^{Neo}$ ES male mouse is also hyper-responsive to cocaine psychomotor effects, in line with the "plasticity alleles" hypothesis (Belsky and Beaver, 2011), and extend its overall risk of developing psychopathology beyond aggressive behavior (Frau et al., 2019a; Godar et al., 2019). This has the unique translational advantage of unveiling the underpinnings of the actions of such a heavily-abused substance in an at-risk segment of population where the interplay of this gene with lifetime stress increases the predisposition to progress into a SUD (Fite et al., 2018, 2020; Stogner and Gibson, 2013; Vanyukov et al., 2004, 2007). This mouse model recapitulates a complex GxE interaction producing long-lasting brain adaptations in monoaminergic systems (Frau et al., 2019a; Godar et al., 2019), heavily implicated in cocaine's rewarding actions. Indeed, MAOA$^{Neo}$ ES mouse VTA dopamine neurons display increased responsiveness to excitatory stimuli (Frau et al., 2019a), a key neural adaptation contributing to stress effects and to core features of drug addiction (Bellone et al., 2021; Saal et al., 2003).

Our results also substantially extend the observation of a cooperative interaction between 2AG and dopamine in the regulation of GABA transmission on rat VTA dopamine neurons only upon repeated cocaine exposure *in vivo* (Pan et al., 2008a,b) via activation of DAD2 and CB1 receptors (Pan et al., 2009). Hence, in MAOA$^{Neo}$ ES mice, concomitant *in vivo* cocaine administration with either DAD2 or CB1 antagonist prevents cocaine-induced i) reduction of maximal GABAA IPSC amplitude, ii) decreased GABA release probability, iii) DSI expression, and iv) hyperlocomotion. Similarly, in MAOA$^{Neo}$ ES mice, concomitant *in vivo* cocaine treatment with MAGL inhibitor JZL184, by presumably enhancing 2AG levels, occludes cocaine effects on GABA synaptic efficacy, DSI and locomotor activity. Collectively, these data indicate that cocaine-induced hyperlocomotion and reduction of GABAergic synaptic efficacy and DSI in VTA dopamine cells share common mechanisms and molecular targets for both cocaine and 2AG, which involve DAD2 and CB1 receptor activation.

Remarkably, repeated *in vivo* cocaine exposure enables a 2AG-mediated DSI, expressed by VTA dopamine neurons only in MAOA$^{Neo}$ ES mice that cannot be ascribed to a larger number of CB1Rs, or a greater effect produced upon their activation. Conversely, the observation that 2AG phasic signal is enhanced in either time and/or space at these inhibitory afferents impinging upon VTA dopamine neurons is consistent with previous reports showing that DSI strength is determined by 2AG degradation rate (Melis et al., 2013, 2014; Pan et al., 2009; Santoni et al., 2023; Yoshida et al., 2011). Since MAOA$^{Neo}$ ES mouse dopamine neurons *per se* do not express DSI (Fig. 4), it is important to elucidate how cocaine, when repeatedly administered, affects sensitivity and/or activity and/or expression of MAGL exclusively in MAOA$^{Neo}$ ES mice. Of note, the observation that the effects of *in vitro* application and *in vivo* administration of JZL184 overlap, being DSI magnitude and time-course similarly expressed in all experimental groups under both experimental conditions, supports the evidence that when DSI is already expressed JZL184 causes decrements in 2AG-dependent plasticity, CB1R down-regulation and desensitization (Schlosburg et al., 2010).

On the one hand, our results are in contrast with previous reports in C57Bl6/J mice (Blanco et al., 2014, 2016; Palomino et al., 2014). On the other hand, one must point out that genetic mouse background, cocaine dose and regimen duration, and brain regions examined differ from ours, which might help resolve these discrepancies. Nonetheless, it is worth noting that a similar phenomenon is associated with innate alcohol preference (Melis et al., 2014) and a faster acquisition in cannabinoid-self administration (Melis et al., 2013). Since not only DSI transiently silences inhibitory inputs onto dopamine cells, but also increases their responsiveness to excitatory stimuli, one might speculate that it might prime them for subsequent plasticity induction associated to vulnerability traits to some behavioral actions of abused drugs.

Several limitations of our study should be acknowledged. First, our behavioral analysis for the susceptibility to cocaine effects is curtailed to cocaine-induced hyperlocomotion. Second, our recordings were carried out from putative dopamine neurons within the lateral portion of the VTA, which largely projects to Nucleus Accumbens lateral shell (Lammel et al., 2011), so it is likely that these putative dopamine neurons would mainly project to this region. Third, besides blocking membrane transporters for dopamine, cocaine also blocks the uptake of serotonin and norepinephrine, as well as ligand- and voltage-gated channels (Uhl et al., 2002). Fourth, this study only examines pre-adolescent age and no other sensitive developmental windows. Fifth, only one dose of cocaine was assessed. Sixth, the mice were passively rather actively exposed to cocaine (Jacobs et al., 2003). Seventh, this investigation was carried out in males only. Finally, since cocaine pharmacokinetic profile is not available for MAOA$^{Neo}$ mice, we cannot rule out differences in drug metabolism.

These limitations notwithstanding, our results gain insights into the mechanisms influencing the overall risk for cocaine use disorder, and identify molecular targets (i.e., DAD2, CB1, MAGL) that could prove effective in age-specific management of this disorder.

## 5. Conclusions

In conclusion, our findings provide evidence that multifactorial conditions driven by specific genetic ($MAOA^{Neo}$), biological (age), and environmental (ES, cocaine) influences can produce profound molecular alterations leading to reduced inhibition of dopamine cells, and enhanced 2AG-mediated signaling at these synapses that have important behavioral associations, including vulnerability to cocaine actions.

## Authors contribution

V.S. and S.A. performed behavioral experiments and analyzed the data. V.S. carried out the electrophysiological recordings, analyzed the corresponding data and prepared the figures. R.F and M.B. reviewed the manuscript. M.B. provided the animals. M.M. conceived, designed and supervised the project, provided funding and wrote the manuscript.

## Funding

The present study was supported by the Region of Sardinia (RASSR32909 to M.M.) and the University of Cagliari (RICCAR 2017 and 2018 to M.M.).

## CRediT authorship contribution statement

**Valeria Serra:** performed behavioral experiments and analyzed the data, carried out the electrophysiological recordings, analyzed the corresponding data and prepared the figures. **Sonia Aroni:** performed behavioral experiments and analyzed the data. **Marco Bortolato:** Writing – review & editing, provided the animals. **Roberto Frau:** Writing – review & editing. **Miriam Melis:** Conceptualization, Methodology, Supervision, the project, provided funding and wrote the manuscript.

## Declaration of competing interest

The authors have nothing to disclose.

## Data availability

Data will be made available on request.

## Acknowledgements

The authors thank F. Traccis, S. Aramo, and the CeSASt personnel for their skillful assistance.

## References

Administration SAMHSA, 2014. The TEDS Report: Age of Substance Use Initiation Among Treatment Admissions Aged 18 to 30.

Administration SAMHSA, 2018. Key Substance Use and Mental Health Indicators in the United States: Results from the 2018 National Survey on Drug Use and Health.

Alia-Klein, N., Goldstein, R.Z., Kriplani, A., Logan, J., Tomasi, D., Williams, B., Telang, F., Shumay, E., Biegon, A., Craig, I.W., Henn, F., Wang, G.-J., Volkow, N.D., Fowler, J. S., 2008. Brain monoamine oxidase A activity predicts trait aggression. J. Neurosci. 28, 5099–5104. https://doi.org/10.1523/JNEUROSCI.0925-08.2008.

Alia-Klein, N., Parvaz, M.A., Woicik, P.A., Konova, A.B., Maloney, T., Shumay, E., Wang, R., Telang, F., Biegon, A., Wang, G.-J., Fowler, J.S., Tomasi, D., Volkow, N.D., Goldstein, R.Z., 2011. Gene by disease interaction on orbitofrontal gray matter in cocaine addiction. Arch. Gen. Psychiatr. 68, 283–294. https://doi.org/10.1001/archgenpsychiatry.2011.10.

Aliczki, M., Varga, Z.K., Balogh, Z., Haller, J., 2015. Involvement of 2-arachidonoylglycerol signaling in social challenge responding of male CD1 mice. Psychopharmacology 232, 2157–2167.

Alves, R.L., Oliveira, P., Lopes, I.M., Portugal, C.C., Alves, C.J., Barbosa, F., Summavielle, T., Magalhães, A., 2020. Early-life stress affects drug abuse susceptibility in adolescent rat model independently of depression vulnerability. Sci. Rep. 10, 13326 https://doi.org/10.1038/s41598-020-70242-4.

Amsterdam, J. van, Talhout, R., Vleeming, W., Opperhuizen, A., 2006. Contribution of monoamine oxidase (MAO) inhibition to tobacco and alcohol addiction. Life Sci. 79, 1969–1973. https://doi.org/10.1016/j.lfs.2006.06.010.

Andersen, S.L., 2005. Stimulants and the developing brain. Trends Pharmacol. Sci. 26, 237–243. https://doi.org/10.1016/j.tips.2005.03.009.

Bellone, C., Loureiro, M., Lüscher, C., 2021. Drug-evoked synaptic plasticity of excitatory transmission in the ventral tegmental area. Cold Spring Harb Perspect Med 11, a039701. https://doi.org/10.1101/cshperspect.a039701.

Belsky, J., Beaver, K.M., 2011. Cumulative-genetic plasticity, parenting and adolescent self-regulation. JCPP (J. Child Psychol. Psychiatry) 52, 619–626. https://doi.org/10.1111/j.1469-7610.2010.02327.x.

Blanco, E., Pavón, F.J., Palomino, A., Luque-Rojas, M.J., Serrano, A., Rivera, P., Bilbao, A., Alen, F., Vida, M., Suárez, J., Rodríguez de Fonseca, F., 2014. Cocaine-induced behavioral sensitization is associated with changes in the expression of endocannabinoid and glutamatergic signaling systems in the mouse prefrontal cortex. Int. J. Neuropsychopharmacol. 18 https://doi.org/10.1093/ijnp/pyu024 pyu024.

Blanco, E., Galeano, P., Palomino, A., Pavón, F.J., Rivera, P., Serrano, A., Alen, F., Rubio, L., Vargas, A., Castilla-Ortega, E., Decara, J., Bilbao, A., de Fonseca, F.R., Suárez, J., 2016. Cocaine-induced behavioral sensitization decreases the expression of endocannabinoid signaling-related proteins in the mouse hippocampus. Eur. Neuropsychopharmacol 26, 477–492. https://doi.org/10.1016/j.euroneuro.2015.12.040.

Blankman, J.L., Simon, G.M., Cravatt, B.F., 2007. A comprehensive profile of brain enzymes that hydrolyze the endocannabinoid 2-arachidonoylglycerol. Chem. Biol. 14, 1347–1356. https://doi.org/10.1016/j.chembiol.2007.11.006.

Bocklisch, C., Pascoli, V., Wong, J.C.Y., House, D.R.C., Yvon, C., de Roo, M., Tan, K.R., Lüscher, C., 2013. Cocaine disinhibits dopamine neurons by potentiation of GABA transmission in the ventral tegmental area. Science 341, 1521–1525. https://doi.org/10.1126/science.1237059.

Borgland, S.L., Malenka, R.C., Bonci, A., 2004. Acute and chronic cocaine-induced potentiation of synaptic strength in the ventral tegmental area: electrophysiological and behavioral correlates in individual rats. J. Neurosci. 24, 7482–7490. https://doi.org/10.1523/JNEUROSCI.1312-04.2004.

Bortolato, M., Chen, K., Godar, S.C., Chen, G., Wu, W., Rebrin, I., Farrell, M.R., Scott, A. L., Wellman, C.L., Shih, J.C., 2011. Social deficits and perseverative behaviors, but not overt aggression, in MAO-A hypomorphic mice. Neuropsychopharmacology 36, 2674–2688. https://doi.org/10.1038/npp.2011.157.

Brady, K.T., Myrick, H., McElroy, S., 1998. The relationship between substance use disorders, impulse control disorders, and pathological aggression. Am. J. Addict. 7, 221–230. https://doi.org/10.1111/j.1521-0391.1998.tb00340.x.

Brake, W.G., Zhang, T.Y., Diorio, J., Meaney, M.J., Gratton, A., 2004. Influence of early postnatal rearing conditions on mesocorticolimbic dopamine and behavioural responses to psychostimulants and stressors in adult rats. Eur. J. Neurosci. 19, 1863–1874. https://doi.org/10.1111/j.1460-9568.2004.03286.x.

Cabib, S., Castellano, C., Cestari, V., Filibeck, U., Puglisi-Allegra, S., 1991. D1 and D2 receptor antagonists differently affect cocaine-induced locomotor hyperactivity in the mouse. Psychopharmacology 105, 335–339.

Caspi, A., McClay, J., Moffitt, T.E., Mill, J., Martin, J., Craig, I.W., Taylor, A., Poulton, R., 2002. Role of genotype in the cycle of violence in maltreated children. Science 297, 851–854. https://doi.org/10.1126/science.1072290.

Castro-Zavala, A., Martín-Sánchez, A., Valverde, O., 2020. Sex differences in the vulnerability to cocaine's addictive effects after early-life stress in mice. Eur. Neuropsychopharmacol 32, 12–24. https://doi.org/10.1016/j.euroneuro.2019.12.112.

Castro-Zavala, A., Martín-Sánchez, A., Luján, M.Á., Valverde, O., 2021. Maternal separation increases cocaine intake through a mechanism involving plasticity in glutamate signalling. Addiction Biol. 26, e12911 https://doi.org/10.1111/adb.12911.

Checknita, D., Maussion, G., Labonté, B., Comai, S., Tremblay, R.E., Vitaro, F., Turecki, N., Bertazzo, A., Gobbi, G., Côté, G., Turecki, G., 2015. Monoamine oxidase a gene promoter methylation and transcriptional downregulation in an offender population with antisocial personality disorder. Br. J. Psychiatr. 206, 216–222. https://doi.org/10.1192/bjp.bp.114.144964.

Delavari, F., Sheibani, V., Esmaeili-Mahani, S., Nakhaee, N., 2016. Maternal separation and the risk of drug abuse in later life. Addict Health 8, 107–114.

Enoch, M.-A., 2011. The role of early life stress as a predictor for alcohol and drug dependence. Psychopharmacology (Berl) 214, 17–31. https://doi.org/10.1007/s00213-010-1916-6.

Ernst, M., Luciana, M., 2015. Neuroimaging of the dopamine/reward system in adolescent drug use. CNS Spectr. 20, 427–441.

ESPAD, 2020. ESPAD Report 2019: Results from the European School Survey Project on Alcohol and Other Drugs. EMCDDA Joint Publications.

Fernàndez-Castillo, N., Cabana-Domínguez, J., Corominas, R., Cormand, B., 2022. Molecular genetics of cocaine use disorders in humans. Mol. Psychiatr. 27, 624–639. https://doi.org/10.1038/s41380-021-01256-1.

Fite, P.J., Brown, S., Hossain, W., Manzardo, A., Butler, M.G., Bortolato, M., 2018. Tobacco and cannabis use in college students are predicted by sex-dimorphic interactions between MAOA genotype and child abuse. CNS Neurosci. Ther. 25, 101–111. https://doi.org/10.1111/cns.13002.

Fite, P.J., Brown, S., Hossain, W.A., Manzardo, A., Butler, M.G., Bortolato, M., 2020. Sex-Dimorphic interactions of MAOA genotype and child maltreatment predispose college students to polysubstance use. Front. Genet. 10.

Fowler, J.S., Volkow, N.D., Wang, G.-J., Pappas, N., Logan, J., Shea, C., Alexoff, D., MacGregor, R.R., Schlyer, D.J., Zezulkova, I., Wolf, A.P., 1996. Brain monoamine

oxidase A inhibition in cigarette smokers. Proc. Natl. Acad. Sci. USA 93, 14065–14069. https://doi.org/10.1073/pnas.93.24.14065.
Fowler, J.S., Alia-Klein, N., Kriplani, A., Logan, J., Williams, B., Zhu, W., Craig, I.W., Telang, F., Goldstein, R., Volkow, N.D., Vaska, P., Wang, G.-J., 2007. Evidence that brain MAO A activity does not correspond to MAO A genotype in healthy male subjects. Biol. Psychiatr. 62, 355–358. https://doi.org/10.1016/j.biopsych.2006.08.038.
Frau, R., Fanni, S., Serra, V., Simola, N., Godar, S.C., Traccis, F., Devoto, P., Bortolato, M., Melis, M., 2019a. Dysfunctional mesocortical dopamine circuit at pre-adolescence is associated to aggressive behavior in MAO-A hypomorphic mice exposed to early life stress. Neuropharmacology, The Neuropharmacology of Social Behavior: From Bench to Bedside 159, 107517. https://doi.org/10.1016/j.neuropharm.2019.01.032.
Frau, R., Miczán, V., Traccis, F., Aroni, S., Pongor, C.I., Saba, P., Serra, V., Sagheddu, C., Fanni, S., Congiu, M., Devoto, P., Cheer, J.F., Katona, I., Melis, M., 2019b. Prenatal THC exposure produces a hyperdopaminergic phenotype rescued by pregnenolone. Nat. Neurosci. 22, 1975–1985. https://doi.org/10.1038/s41593-019-0512-2.
Ganguly, P., Honeycutt, J.A., Rowe, J.R., Demaestri, C., Brenhouse, H.C., 2019. Effects of early life stress on cocaine conditioning and AMPA receptor composition are sex-specific and driven by TNF. Brain Behav. Immun. 78, 41–51. https://doi.org/10.1016/j.bbi.2019.01.006.
Godar, S.C., Mosher, L.J., Scheggi, S., Devoto, P., Moench, K.M., Strathman, H.J., Jones, C.M., Frau, R., Melis, M., Gambarana, C., Wilkinson, B., DeMontis, M.G., Fowler, S.C., Coba, M.P., Wellman, C.L., Shih, J.C., Bortolato, M., 2019. Gene-environment interactions in antisocial behavior are mediated by early-life 5-HT2A receptor activation. Neuropharmacology 159, 107513. https://doi.org/10.1016/j.neuropharm.2019.01.028.
Grant, B.F., 1998. Age at smoking onset and its association with alcohol consumption and DSM-IV alcohol abuse and dependence: results from the National Longitudinal Alcohol Epidemiologic Survey. J. Subst. Abuse 10, 59–73. https://doi.org/10.1016/s0899-3289(99)80141-2.
Grant, B.F., Dawson, D.A., 1998. Age of onset of drug use and its association with DSM-IV drug abuse and dependence: results from the National Longitudinal Alcohol Epidemiologic Survey. J. Subst. Abuse 10, 163–173. https://doi.org/10.1016/s0899-3289(99)80131-x.
Guo, G., Ou, X.-M., Roettger, M., Shih, J.C., 2008. The VNTR 2 repeat in MAOA and delinquent behavior in adolescence and young adulthood: associations and MAOA promoter activity. Eur. J. Hum. Genet. 16, 626–634. https://doi.org/10.1038/sj.ejhg.5201999.
Hanson, J.L., Williams, A.V., Bangasser, D.A., Peña, C.J., 2021. Impact of early life stress on reward circuit function and regulation. Front. Psychiatr. 12.
Howell, L.L., Kimmel, H.L., 2008. Monoamine transporters and psychostimulant addiction. Biochem. Pharmacol. 75, 196–217. https://doi.org/10.1016/j.bcp.2007.08.003.
Jacobs, E.H., Smit, A.B., de Vries, T.J., Schoffelmeer, A.N., 2003. Neuroadaptive effects of active versus passive drug administration in addiction research. Trends Pharmacol. Sci. 24, 566–573.
Jordan, C.J., Andersen, S.L., 2016. Sensitive periods of substance abuse: early risk for the transition to dependence. Dev Cogn Neurosci 25, 29–44. https://doi.org/10.1016/j.dcn.2016.10.004.
Kreek, M.J., Bart, G., Lilly, C., Laforge, K.S., Nielsen, D.A., 2005. Pharmacogenetics and human molecular genetics of opiate and cocaine addictions and their treatments. Pharmacol. Rev. 57, 1–26. https://doi.org/10.1124/pr.57.1.1.
Lammel, S., Ion, D.I., Roeper, J., Malenka, R.C., 2011. Projection-specific modulation of dopamine neuron synapses by aversive and rewarding stimuli. Neuron 70, 855–862. https://doi.org/10.1016/j.neuron.2011.03.025.
Lea, R., Chambers, G., 2007. Monoamine oxidase, addiction, and the "warrior" gene hypothesis. N. Z.Med. J. 120, U2441.
Liu, Q., Pu, L., Poo, M., 2005. Repeated cocaine exposure in vivo facilitates LTP induction in midbrain dopamine neurons. Nature 437, 1027–1031. https://doi.org/10.1038/nature04050.
Lo Iacono, L., Catale, C., Martini, A., Valzania, A., Viscomi, M.T., Chiurchiù, V., Guatteo, E., Bussone, S., Perrone, F., Di Sabato, P., Aricò, E., D'Argenio, A., Troisi, A., Mercuri, N.B., Maccarrone, M., Puglisi-Allegra, S., Casella, P., Carola, V., 2018. From traumatic childhood to cocaine abuse: the critical function of the immune system. Biological Psychiatry, Cocaine Addiction, Obsessive-Compulsive Disorder, and Corticostriatal Plasticity 84, 905–916. https://doi.org/10.1016/j.biopsych.2018.05.022.
Long, J.Z., Li, W., Booker, L., Burston, J.J., Kinsey, S.G., Schlosburg, J.E., Pavon, F.J., Serrano, A.M., Selley, D.E., Parsons, L.H., Lichtman, A.H., Cravatt, B.F., 2009. Selective blockade of 2-arachidonoylglycerol hydrolysis produces cannabinoid behavioral effects. Nat. Chem. Biol. 5, 37–44.
Luciana, M., Wahlstrom, D., Porter, J.N., Collins, P.F., 2012. Dopaminergic modulation of incentive motivation in adolescence: age-related changes in signaling, individual differences, and implications for the development of self-regulation. Dev. Psychol. 48, 844–861.
Mannuzza, S., Klein, R.G., Moulton, J.L., 2008. Lifetime criminality among boys with ADHD: a prospective follow-up study into adulthood using official arrest records. Psychiatr. Res. 160, 237–246. https://doi.org/10.1016/j.psychres.2007.11.003.
McCutcheon, J.E., Marinelli, M., 2009. Age matters. Eur. J. Neurosci. 29, 997–1014.
McCutcheon, J.E., Conrad, K.L., Carr, S.B., Ford, K.A., McGehee, D.S., Marinelli, M., 2012. Dopamine neurons in the ventral tegmental area fire faster in adolescent rats than in adults. J. Neurophysiol. 108, 1620–1630.
Melis, M., Pistis, M., 2012. Hub and switches: endocannabinoid signalling in midbrain dopamine neurons. Philos. Trans. R. Soc. Lond. Ser. B Biol. Sci. 367, 3276–3285.
Melis, M., Camarini, R., Ungless, M.A., Bonci, A., 2002. Long-lasting potentiation of GABAergic synapses in dopamine neurons after a single in vivo ethanol exposure. J. Neurosci. 22, 2074–2082. https://doi.org/10.1523/JNEUROSCI.22-06-02074.2002.
Melis, M., Pistis, M., Perra, S., Muntoni, A.L., Pillolla, G., Gessa, G.L., 2004. Endocannabinoids mediate presynaptic inhibition of glutamatergic transmission in rat ventral tegmental area dopamine neurons through activation of CB1 receptors. J. Neurosci. 24, 53–62. https://doi.org/10.1523/JNEUROSCI.4503-03.2004.
Melis, M., Pillolla, G., Perra, S., Colombo, G., Muntoni, A.L., Pistis, M., 2009. Electrophysiological properties of dopamine neurons in the ventral tegmental area of Sardinian alcohol-preferring rats. Psychopharmacology 201, 471–481. https://doi.org/10.1007/s00213-008-1309-2.
Melis, M., De Felice, M., Lecca, S., Fattore, L., Pistis, M., 2013. Sex-specific tonic 2-arachidonoylglycerol signaling at inhibitory inputs onto dopamine neurons of Lister Hooded rats. Front. Integr. Neurosci. 7, 93. https://doi.org/10.3389/fnint.2013.00093.
Melis, M., Sagheddu, C., De Felice, M., Casti, A., Madeddu, C., Spiga, S., Muntoni, A.L., Mackie, K., Marsicano, G., Colombo, G., Castelli, M.P., Pistis, M., 2014. Enhanced endocannabinoid-mediated modulation of rostromedial tegmental nucleus drive onto dopamine neurons in Sardinian alcohol-preferring rats. J. Neurosci. 34, 12716–12724. https://doi.org/10.1523/JNEUROSCI.1844-14.2014.
Miczek, K.A., Covington, H.E., Nikulina, E.M., Hammer, R.P., 2004. Aggression and defeat: persistent effects on cocaine self-administration and gene expression in peptidergic and aminergic mesocorticolimbic circuits. Neuroscience & Biobehavioral Reviews, Foundations and Innovations in the Neuroscience of Drug Abuse 27, 787–802. https://doi.org/10.1016/j.neubiorev.2003.11.005.
Moeller, S.J., Parvaz, M.A., Shumay, E., Wu, S., Beebe-Wang, N., Konova, A.B., Misyrlis, M., Alia-Klein, N., Goldstein, R.Z., 2014. Monoamine polygenic liability in health and cocaine dependence: imaging genetics study of aversive processing and associations with depression symptomatology. Drug Alcohol Depend. 140, 17–24. https://doi.org/10.1016/j.drugalcdep.2014.04.019.
Morales, M., Margolis, E.B., 2017. Ventral tegmental area: cellular heterogeneity, connectivity and behaviour. Nat. Rev. Neurosci. 18, 73–85.
Nair, A.B., Jacob, S., 2016. A simple practice guide for dose conversion between animals and human. J. Basic Clin. Pharm. 7, 27–31.
Palomino, A., Pavón, F.-J., Blanco-Calvo, E., Serrano, A., Arrabal, S., Rivera, P., Alén, F., Vargas, A., Bilbao, A., Rubio, L., Rodríguez de Fonseca, F., Suárez, J., 2014. Effects of acute versus repeated cocaine exposure on the expression of endocannabinoid signaling-related proteins in the mouse cerebellum. Front. Integr. Neurosci. 8, 22. https://doi.org/10.3389/fnint.2014.00022.
Pan, B., Hillard, C.J., Liu, Q., 2008a. Endocannabinoid signaling mediates cocaine-induced inhibitory synaptic plasticity in midbrain dopamine neurons. J. Neurosci. 28, 1385–1397. https://doi.org/10.1523/JNEUROSCI.4033-07.2008.
Pan, B., Hillard, C.J., Liu, Q., 2008b. D2 dopamine receptor activation facilitates endocannabinoid-mediated long-term synaptic depression of GABAergic synaptic transmission in midbrain dopamine neurons via cAMP-protein kinase A signaling. J. Neurosci. 28, 14018–14030. https://doi.org/10.1523/JNEUROSCI.4035-08.2008.
Pan, B., Wang, W., Long, J.Z., Sun, D., Hillard, C.J., Cravatt, B.F., Liu, Q., 2009. Blockade of 2-arachidonoylglycerol hydrolysis by selective monoacylglycerol lipase inhibitor 4-nitrophenyl 4-(Dibenzo[d][1,3]dioxol-5-yl(hydroxy)methyl)piperidine-1-carboxylate (JZL184) enhances retrograde endocannabinoid signaling. J. Pharmacol. Exp. Therapeut. 331, 591–597. https://doi.org/10.1124/jpet.109.158162.
Saal, D., Dong, Y., Bonci, A., Malenka, R.C., 2003. Drugs of abuse and stress trigger a common synaptic adaptation in dopamine neurons. Neuron 37, 577–582. https://doi.org/10.1016/S0896-6273(03)00021-7.
Sagheddu, C., Melis, M., 2015. Individual differences and vulnerability to drug addiction: a focus on the endocannabinoid system. CNS Neurol. Disord.: Drug Targets 14, 502–517.
Sagheddu, C., Muntoni, A.L., Pistis, M., Melis, M., 2015. Endocannabinoid signaling in motivation, reward, and addiction: influences on mesocorticolimbic dopamine function. Int. Rev. Neurobiol. 125, 257–302.
Santo, T., Campbell, G., Gisev, N., Tran, L., Colledge, S., Di Tanna, G.L., Degenhardt, L., 2021. Prevalence of childhood maltreatment among people with opioid use disorder: a Systematic Review and Meta-analysis. Drug Alcohol Depend. 219, 108459 https://doi.org/10.1016/j.drugalcdep.2020.108459.
Santoni, M., Sagheddu, C., Serra, V., Mostallino, R., Castelli, M.P., Pisano, F., Scherma, M., Fadda, P., Muntoni, A.L., Zamberletti, E., Rubino, T., Melis, M., Pistis, M., 2023. Maternal immune activation impairs endocannabinoid signaling in the mesolimbic system of adolescent male offspring. Brain Behav. Immun. 109, 271–284.
Scheidell, J.D., Quinn, K., McGorray, S.P., Frueh, B.C., Beharie, N.N., Cottler, L.B., Khan, M.R., 2018. Childhood traumatic experiences and the association with marijuana and cocaine use in adolescence through adulthood. Addiction 113, 44–56. https://doi.org/10.1111/add.13921.
Schlosburg, J.E., Blankman, J.L., Long, J.Z., Nomura, D.K., Pan, B., Kinsey, S.G., Nguyen, P.T., Ramesh, D., Booker, L., Burston, J.J., Thomas, E.A., Selley, D.E., Sim-Selley, L.J., Liu, Q., Lichtman, A.H., Cravatt, B.F., 2010. Chronic monoacylglycerol lipase blockade causes functional antagonism of the endocannabinoid system. Nat. Neurosci. 13, 1113–1119. https://doi.org/10.1038/nn.2616.
Schlussman, S.D., Ho, A., Zhou, Y., Curtis, A.E., Kreek, M.J., 1998. Effects of "binge" pattern cocaine on stereotypy and locomotor activity in C57BL/6J and 129/J mice. Pharmacol., Biochem. Behav. 60, 593–599. https://doi.org/10.1016/S0091-3057(98)00047-1.
Shumay, E., Logan, J., Volkow, N.D., Fowler, J.S., 2012. Evidence that the methylation state of the monoamine oxidase A (MAOA) gene predicts brain activity of MAOA

enzyme in healthy men. Epigenetics 7, 1151–1160. https://doi.org/10.4161/epi.21976.
Stogner, J., Gibson, C., 2013. Stressful life events and adolescent drug use: moderating influences of the MAOA gene. J. Crim. Justice 41, 357–363. https://doi.org/10.1016/j.jcrimjus.2013.06.003.
Thomsen, M., Caine, S.B., 2011. Psychomotor stimulant effects of cocaine in rats and 15 mouse strains. Exp. Clin. Psychopharmacol 19, 321–341. https://doi.org/10.1037/a0024798.
Tong, J., Liu, X., Vickstrom, C., Li, Y., Yu, L., Lu, Y., Smrcka, A.V., Liu, Q.-S., 2017. The epac-phospholipase cε pathway regulates endocannabinoid signaling and cocaine-induced disinhibition of ventral tegmental area dopamine neurons. J. Neurosci. 37, 3030–3044. https://doi.org/10.1523/JNEUROSCI.2810-16.2017.
Uhl, G.R., Hall, F.S., Sora, I., 2002. Cocaine, reward, movement and monoamine transporters. Mol. Psychiatr. 7, 21–26. https://doi.org/10.1038/sj.mp.4000964.
Ungless, M.A., Whistler, J.L., Malenka, R.C., Bonci, A., 2001. Single cocaine exposure in vivo induces long-term potentiation in dopamine neurons. Nature 411, 583–587. https://doi.org/10.1038/35079077.
Vannan, A., Powell, G.L., Scott, S.N., Pagni, B.A., Neisewander, J.L., 2018. Chapter six - animal models of the impact of social stress on cocaine use disorders. In: Olive, M.F., Tomek, S.E. (Eds.), International Review of Neurobiology, Animal Models for Examining Social Influences on Drug Addiction. Academic Press, pp. 131–169. https://doi.org/10.1016/bs.irn.2018.07.005.
Vanyukov, M.M., Maher, B.S., Devlin, B., Tarter, R.E., Kirillova, G.P., Yu, L.-M., Ferrell, R.E., 2004. Haplotypes of the monoamine oxidase genes and the risk for substance use disorders. Am. J. Med. Genet. Part B: Neuropsychiatric Genetics 125B, 120–125. https://doi.org/10.1002/ajmg.b.20105.
Vanyukov, M.M., Maher, B.S., Devlin, B., Kirillova, G.P., Kirisci, L., Yu, L.-M., Ferrell, R.E., 2007. The MAOA promoter polymorphism, disruptive behavior disorders, and early onset substance use disorder: gene–environment interaction. Psychiatr. Genet. 17, 323. https://doi.org/10.1097/YPG.0b013e32811f6691.
Vaseghi, G., Rabbani, M., Hajhashemi, V., 2012. The CB(1) receptor antagonist, AM281, improves recognition loss induced by naloxone in morphine withdrawal mice. Basic Clin. Pharmacol. Toxicol. 111, 161–165.
Vaseghi, G., Rabbani, M., Hajhashemi, V., 2013. The effect of AM281, a cannabinoid antagonist, on memory performance during spontaneous morphine withdrawal in mice. Res Pharm Sci 8, 59–64.
Verdejo-García, A., Albein-Urios, N., Molina, E., Ching-López, A., Martínez-González, J. M., Gutiérrez, B., 2013. A MAOA gene*cocaine severity interaction on impulsivity and neuropsychological measures of orbitofrontal dysfunction: preliminary results. Drug Alcohol Depend. 133, 287–290. https://doi.org/10.1016/j.drugalcdep.2013.04.031.
Viding, E., Frith, U., 2006. Genes for susceptibility to violence lurk in the brain. Proc. Natl. Acad. Sci. U. S. A. 103, 6085–6086. https://doi.org/10.1073/pnas.0601350103.
Vink, J.M., 2016. Genetics of addiction: future focus on gene × environment interaction? J. Stud. Alcohol Drugs 77, 684–687. https://doi.org/10.15288/jsad.2016.77.684.
Viola, T.W., Wearick-Silva, L.E., De Azeredo, L.A., Centeno-Silva, A., Murphy, C., Marshall, P., Li, X., Singewald, N., Garcia, F., Bredy, T.W., Grassi-Oliveira, R., 2016. Increased cocaine-induced conditioned place preference during periadolescence in maternally separated male BALB/c mice: the role of cortical BDNF, microRNA-212, and MeCP2. Psychopharmacology 233, 3279–3288. https://doi.org/10.1007/s00213-016-4373-z.
Volkow, N.D., Fowler, J.S., Wang, G.-J., Swanson, J.M., Telang, F., 2007. Dopamine in drug abuse and addiction: results of imaging studies and treatment implications. Arch. Neurol. 64, 1575–1579. https://doi.org/10.1001/archneur.64.11.1575.
Weder, N., Yang, B.Z., Douglas-Palumberi, H., Massey, J., Krystal, J.H., Gelernter, J., Kaufman, J., 2009. MAOA genotype, maltreatment, and aggressive behavior: the changing impac of genotype at varying levels of trauma. Biol. Psychiatr. 65 https://doi.org/10.1016/j.biopsych.2008.09.013.
Yoshida, T., Uchigashima, M., Yamasaki, M., Katona, I., Yamazaki, M., Sakimura, K., Kano, M., Yoshioka, M., Watanabe, M., 2011. Unique inhibitory synapse with particularly rich endocannabinoid signaling machinery on pyramidal neurons in basal amygdaloid nucleus. Proc. Natl. Acad. Sci. U. S. A. 108, 3059–3064. https://doi.org/10.1073/pnas.1012875108.
Yu, Q., Teixeira, C.M., Mahadevia, D., Huang, Y.-Y., Balsam, D., Mann, J.J., Gingrich, J. A., Ansorge, M.S., 2014. Dopamine and serotonin signaling during two sensitive developmental periods differentially impact adult aggressive and affective behaviors in mice. Mol. Psychiatr. 19, 688–698. https://doi.org/10.1038/mp.2014.10.
Zhong, P., Wang, W., Pan, B., Liu, X., Zhang, Z., Long, J.Z., Zhang, H.T., Cravatt, B.F., Liu, Q.S., 2014. Monoacylglycerol lipase inhibition blocks chronic stress-induced depressive-like behaviors via activation of mTOR signaling. In: Neuropsychopharmacology: Official Publication of the American College of Neuropsychopharmacology, vol. 39, pp. 1763–1776.